AN ABSTRACT OF THE THESIS OF

Perumal Sarangabany for the degree of Master of Science in Materials Science presented on March 28, 1994.

Title: Polyurethane Impregnated Kevlar 29 Fabric for Coal Transport Railcars

Redacted for Privacy

Abstract approved: _____
Ernest G. Wolff

Stress analysis was performed to determine the maximum stress acting on a railcar coal support-bed, using COSMOS finite element and WFM micromechanics models. The fracture strength of polyurethane impregnated Kevlar 29 fabric, proposed for integration with the railcar structure, was determined experimentally by loading the impregnated coupons in a micro-computer controlled Instron 4505. Procedures to improve the wettability of a Kevlar 29 orthogonal-weave fabric were investigated. Unimpregnated and impregnated coupons of increasing gage lengths were statically tested for tensile strength to check for gage length effect behavior. Fatigue tests were conducted to predict the stress level (endurance limit) below which the impregnated fabric bed can perform without failure for ten years of the service life. The fracture strength of the polyurethane impregnated fabric, after immersion in aqueous solutions of different pH values for seventy-five hours and in ten percent concentrated sulfuric acid solution at 212°F for ten hours, was measured.

Polyurethane Impregnated Kevlar 29 Fabric for Coal Transport Railcars

by

Perumal Sarangabany

A THESIS

submitted to

Oregon State University

in partial fulfillment of

the requirements for the

degree of

Master of Science

Completed March 28, 1994

Commencement June 1994

APPROVED:

Redacted for Privacy

Associate Professor of Mechanical Engineering, in charge of major

Redacted for Privacy

Head of Department of Mechanical Engineering

Redacted for Privacy

Dean of Graduate School

Date thesis was presented March 28,1994

DEDICATION

To my family, friends, and god.

ACKNOWLEDGEMENTS

I wish to thank Dr. Ernest G. Wolff for his advice and guidance in the course of completion of this thesis, as well as for supporting me financially throughout the course of study at OSU.

I also like to thank Dr. Timothy Kennedy for helping me understand concepts concerned with stress analysis of railcar. I am thankful to Mr. Andy Brickman, Civil Engineering Lab, for having granted me permission to use the MTS machine for fatigue testing. I like to thank Dr. Warnes and Dr. Kenney John for their willingness to preside over my thesis defense.

I am very much indebted to my parents, whose love and affection is a great inspiration in the pursuit of excellence. I never will forget the moral support and the monetary help rendered at times of crisis by my fiancé Pavithra.

I am grateful to Keivan Negahbani who was there for me, whenever I needed help. I sincerely thank Sivaramapuram Krishna for all the help he cheerfully offered during my stay in OSU. I like to thank Srinivas Puligilla for saving me lot of time and work by scanning most of the pictures in this thesis. I also like to thank Rao Hejeebu for having let me use his computer. My room-mates, Raman and Rama Krishna, have also been very helpful in the completion of this thesis. Finally I thank my well-wishers, Ravi Kumar, Raj Manickam, Paranthaman, Pugal 'Andy' and all my friends, who are my strength.

TABLE OF CONTENTS

LIST OF FIGURES

LIST OF TABLES

LIST OF APPENDICES

POLYURETHANE IMPREGNATED KEVLAR 29 FABRIC FOR COAL TRANSPORT RAILCARS

1. INTRODUCTION

Weight saving is an important criterion in the design of railcars for the transportation of coal, mineral ores, gravel, and similar materials. A reduction in the structural weight of the railcar would allow an increase in the coal carrying capacity for the same gross train weight. Fabricating the car body from wrought aluminum which has good corrosion resistance and the car underframe from steel which has high strength, provides a savings in weight of approximately 15,000 lb over conventional all steel cars at competitive cost [1]. Complete replacement of steel structures with less dense materials is not possible because of the required toughness, strength and fatigue resistance. However, the promise that the fabric reinforced composites pose in the load bearing applications and their superiority over other materials (e.g. metals) on a strength-to-weight or stiffness-to-weight basis, suggest an additional weight saving in the railcar by replacing the aluminum coal support-bed. For aircraft, rockets and other applications wherein stiffness-to-weight is the major consideration, graphite has become the dominant, if not exclusive material. Where tensile strength-to-weight is the major consideration, aramid is the chosen one [2].

In the design of fabric reinforced composites deliberate efforts are made in choosing a suitable fabric weave pattern, fiber type, and processing conditions during manufacture so that optimum performance for the final composite is obtained. The forming of textile preforms requires knowledge of the structure of yarns and fibers. Yarns (figure 1) are linear assemblages of

fibers formed into continuous strands having textile characteristics, i.e., substantial strength and flexibility. A yarn may consist of a single or multiple continuous fibers, or short fibers, where a substantial amount of twist or entanglement is needed to overcome fiber slippage. The major textile forming techniques for composites reinforcement are weaving, knitting, braiding, and stitching (figure 2). Woven fabric which offers versatile properties such as high-impact resistance, better toughness, shapability, dimensional stability, and low manufacturing cost is considered for this application. Woven fabrics are formed on a loom by interlacing two or more sets of yarns at right angles. The longitudinal yarns are known as the warp, and the widthwise yarns are known as the filling or weft. The individual yarns in the warp and filling directions are also called an end and a pick, respectively. Depending upon the pattern of yarn interlacing, the fabric is denoted as plain, twill, or satin weave (figure 3). The plain weave fabric is the simplest form of orthogonal woven fabric and it is the form often used in coated-fabric structures [3, 4]. Woven fabrics of Kevlar 29 aramid have a balance of properties generally unattainable with traditional textile fibers or with fiberglass. They also have a balance of tensile and tear strength superior to that attainable with other organic fibers, thus eliminating the necessity to over-construct fabrics to obtain high tear strength.

Kevlar 29 is one form of Kevlar (registered trade mark for one member of DuPont's family of aromatic polyamide fibers; Nomex is also included in this generic fiber category) that has been granted the generic name "aramid" by the Federal Trade Commission. Aramid fibers are aromatic polyamide fibers in which at least 85% of the amide linkages are attached directly to two aromatic rings (figure 4) [5]. Kevlar 29, which is basically poly(p-phenylene teraphthalamide) (PPTA), has a tensile strength of 400,000 lb/in^2 and modulus

of 9 million lb/in^2, and is especially suited for a number of applications including ropes, cables, protective clothing, and coated fabrics [6]. The tensile strength of Kevlar 29 is more than twice that of nylon, 15% than that of E-glass, and 60% greater than that of steel (wrought steel, AISI 8760). Kevlar 29 also has high toughness which yields good textile processibility and high impact strength. However, to withstand tear, wear, abrasion, and chemical attack in this application, the Kevlar 29 fabric needs to be impregnated with a resin matrix that can provide these properties.

Polyurethane thermoset systems are widely used in composite applications that require high strength and resiliency. These products provide excellent abrasion resistance, flexibility, hardness, and chemical and solvent resistance; light sensitivity and weatherability are excellent. Raw materials include polyisocyanates and coreactants, e.g. polyester and polyether polyol. The two component systems are prepared by mixing a polyisocyanate with a polyol before application to the substrate. Upon mixing, the isocyanate and polyol react immediately resulting in continual viscosity buildup and eventual gelation.

In choosing a fabric for structural application, knowledge of the stresses acting on the structure due to a given load is essential. Fabrics of required warp and fill tensile strength can then be acquired. Thus a stress analysis of the coal support-bed was performed incorporating the mechanical properties of the materials replacing aluminum. A detailed study was done on the improvement of fabric wettability using an economical impregnation method. Some of the properties such as tensile strength, fatigue life and chemical resistance were characterized to determine the feasibility of using polyurethane impregnated Kevlar 29 fabric as the railcar coal support-bed.

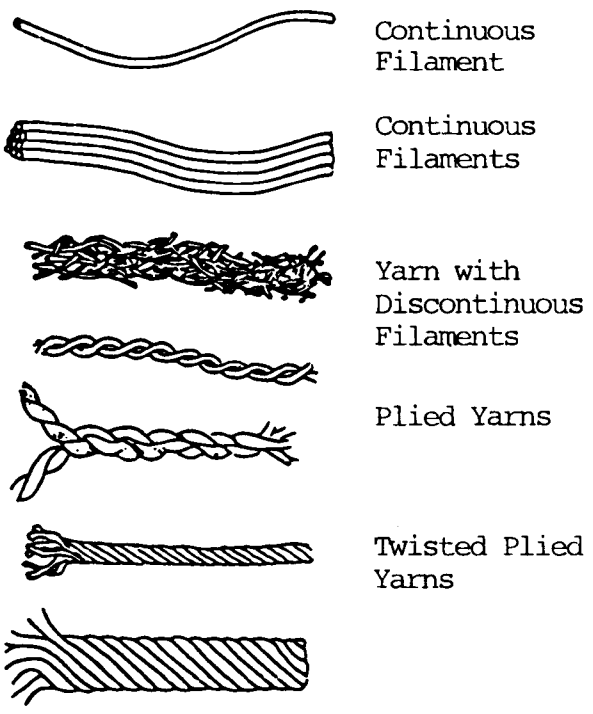

FIGURE 1: IDEALIZED MODELS OF VARIOUS YARN STRUCTURES

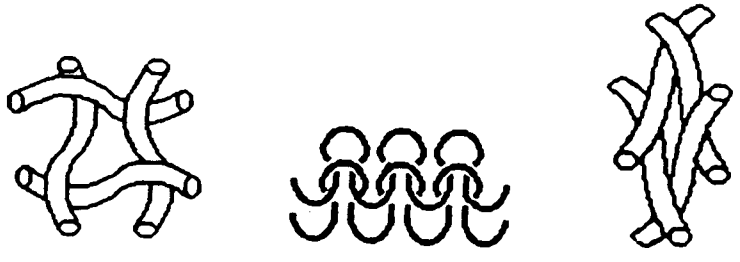

FIGURE 2: BASIC FABRIC STRUCTURES

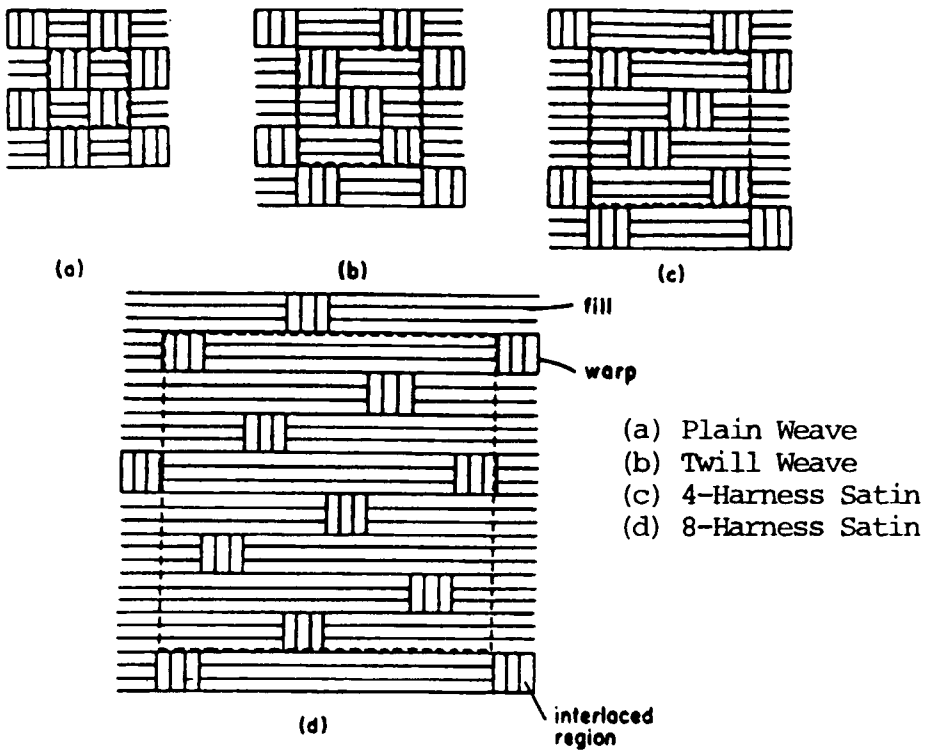

FIGURE 3: WOVEN FABRIC PATTERNS

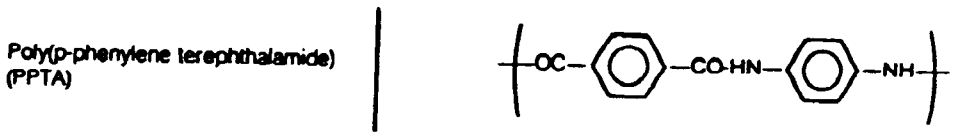

FIGURE 4: CHEMICAL STRUCTURE OF PPTA

2. BACKGROUND

2.1 Stress Analysis of Railcar Floor

Theoretical stress analysis is indispensable as it is very essential to know the strength of the impregnated fabric to be used as the bed in the coal-car (refer figure 5). This requires knowledge of the fabric composite stiffness properties. Mechanical properties data, available in the literature, are mostly for fiber, resin, or a unidirectional lamina. It is very rare to find mechanical properties for fabric or impregnated fabric. However, there are theoretical models [7] which can predict the thermomechanical properties of fabric composites. The three models, developed by Chou and Ishikawa [7] are the mosaic model, the crimp (fiber undulation) model and the bridging model. The mosaic model gives a rough estimation of fabric composite stiffness properties. The bridging model offers better predictability than the other two models, but only in the case of evaluating the elastic properties of satin weaves. Hence, the crimp model which is better than both the mosaic and the bridging models in predicting the elastic properties of plain and twill weaves [8], is used in this study. The stiffness properties, thus calculated for the impregnated fabric, are used for determining the maximum stress acting upon the coal support-bed. The stress analysis is done using Finite Element Methods (FEM). Brief explanation of the calculations involved in the crimp model and FEM is given below:

THE CRIMP MODEL: The classical laminate plate theory is the basis of calculation in all the three models. According to this theory, the membrane stress resultants and moment resultants are given as:

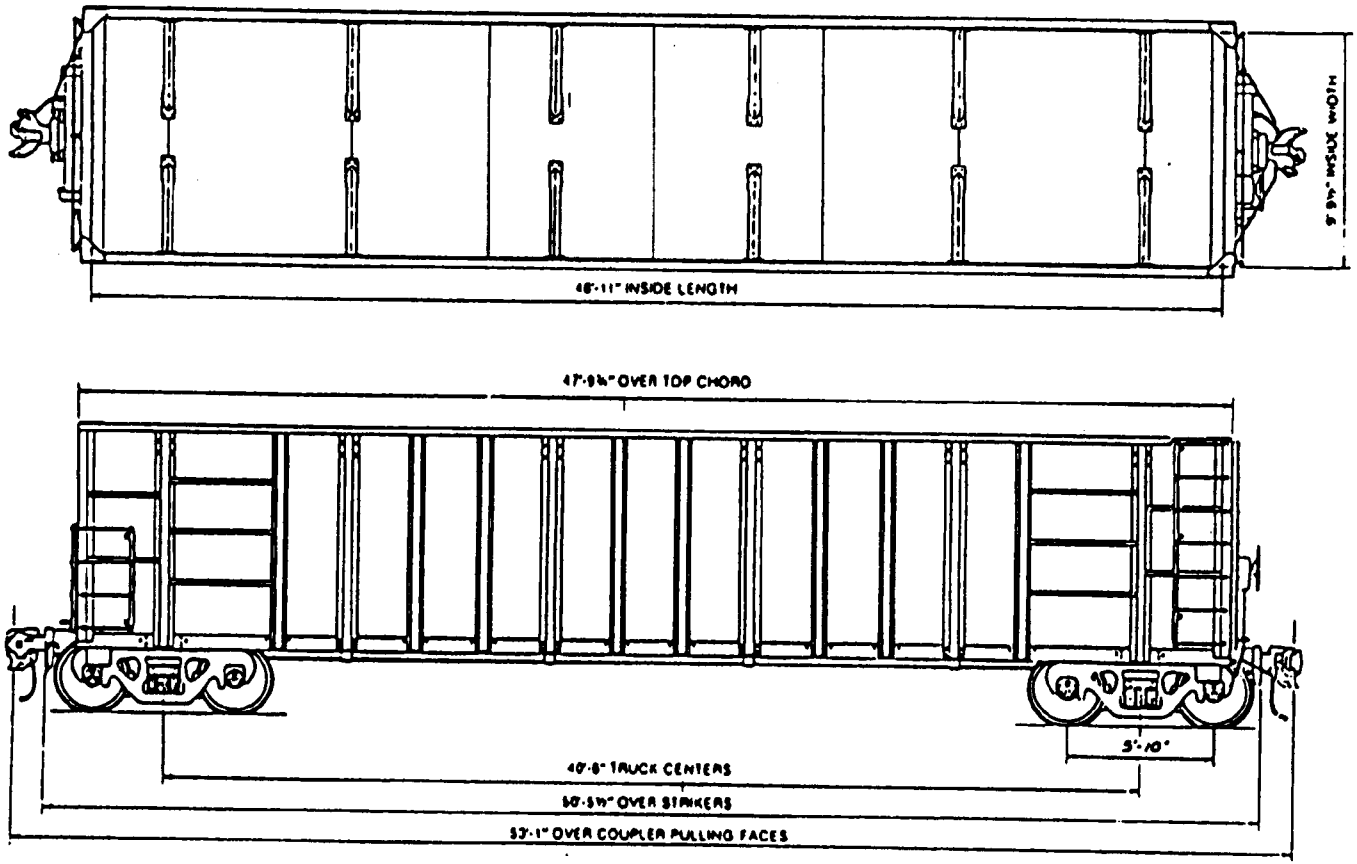

FIGURE 5: COAL-CAR LAYOUT

$$\{N\} = [A]\{\varepsilon_0\} + [B]\{\kappa\}$$
$$\{M\} = [B]\{\varepsilon_0\} + [D]\{\kappa\} \qquad (1)$$

Where N and M are membrane stress resultants and moment resultants respectively, A, B and D are components of stiffness matrix, and ε_0 and κ are strain and curvature of the laminate geometric midplane respectively.

Equations (1) can be rewritten as follows:

$$\begin{Bmatrix} N_i \\ M_i \end{Bmatrix} = \begin{bmatrix} A_{ij} & B_{ij} \\ B_{ij} & D_{ij} \end{bmatrix} \begin{Bmatrix} \varepsilon_0 \\ \kappa_j \end{Bmatrix} (i, j = 1,2, \text{ and } 6) \qquad (2)$$

The subscripts 1, 2, and 6 represent, in the xyz coordinate system, the x direction, the y direction, and the xy plane, respectively. The components of stiffness matrix, A, B and D, are evaluated by integrating through the plate thickness in the Z direction as given below:

$$A_{ij} = \sum_{k=1}^{N} (Q_{ij})_k (h_k - h_{k-1})$$
$$B_{ij} = \sum_{k=1}^{N} (Q_{ij})_k \frac{1}{2}\left(h_k^2 - h_{k-1}^2\right) \qquad (3)$$
$$D_{ij} = \sum (Q_{ij})_k \frac{1}{3}\left(h_k^3 - h_{k-1}^3\right)$$

where Q_{ij} is the lamina stiffness constant that corresponds to the lamina defined by h_k and h_{k-1} in the thickness direction.

The Crimp model considers continuity and undulation of the fibers for the evaluation of stiffness matrix components. For example:

$$A_{ij}(x) = \int_{-h/2}^{h_1(x)-h_t/2} \overset{M}{Q}_{ij}\, dz + \int_{h_1(x)-h_t/2}^{h_1(x)} \overset{F}{Q}_{ij}(\theta) dz$$
$$+ \int_{h_1(x)}^{h_2(x)} \overset{W}{Q}_{ij} dz + \int_{h_2(x)}^{h_t/2} \overset{M}{Q}_{ij}\, dz \qquad (4)$$

where M, F, and W represent matrix, fill yarn, and warp yarn respectively, and $h_1(x)$ and $h_2(x)$ are the parameters that define the undulation shape [4]. The parameters $h_1(x)$ and $h_2(x)$ are described in figure 6. The lamina stiffness constants, pertaining to the fill yarn, $Q^F{}_{ij}(\theta)$ in the above equation, are evaluated as a function of local off-axis angle, $\theta(x)$ defined as:

$$\theta(x) = \arctan\left(\frac{dh_1(x)}{dx}\right) \tag{5}$$

Equation **(3)** is then inverted to obtain an equation of the form given below:

$$\begin{Bmatrix} \varepsilon_0 \\ \kappa \end{Bmatrix} = \begin{bmatrix} A' & B' \\ B'^T & D' \end{bmatrix} \begin{Bmatrix} N \\ M \end{Bmatrix} \tag{6}$$

where $A' = A^{-1} + A^{-1}B(D - BA^{-1}B)BA^{-1}$

$B' = -(A^{-1}B)(D - BA^{-1}B)$

$D' = (D - BA^{-1}B)$

For a single layer of the weave fabric composite, due to the asymmetry of the distribution and properties of the constituent materials of the interlacing structure in the fabrics, the coupling stiffness matrix B is not equal to zero. Therefore, there exists the local coupling effect between in- and out-of-plane deformation. Hence in the crimp model, two conditions namely local warping constrained and local warping allowed, are available to evaluate respectively the upper and lower bounds of elastic constants of the lamina. For design purposes, the local warping allowed condition, which predicts the lower bound of elastic constants, is chosen in this study. Under the local warping allowed condition, the following equations must hold good:

$$\{M\} = 0, \{\kappa\} \neq 0 \tag{7}$$

Therefore eqn. (6) becomes

$$\{\varepsilon_0\} = \mathbf{A}'\{\mathbf{N}\} \tag{8}$$

and the corresponding macroscopical in-plane compliance matrix will be

$$\left[\mathbf{a}^{**}\right] = \mathbf{A}' = \mathbf{A}^{-1} + \mathbf{A}^{-1}\mathbf{B}\left(\mathbf{D} - \mathbf{B}\mathbf{A}^{-1}\mathbf{B}\right)\mathbf{B}\mathbf{A}^{-1} \tag{9}$$

The compliance matrix [a**] is a function of coordinate (x, y) at the representative volume element shown in figure 7. Hence the averaged in-plane compliance over this element can be calculated as given below:

$$\left[\bar{\mathbf{a}}\right] = \frac{1}{\mathbf{ab}} \int_{-a/2}^{a/2} \int_{-b/2}^{b/2} \left[\mathbf{a}^{*}\right] \mathbf{or} \left[\mathbf{a}^{**}\right] \mathbf{dxdy} \tag{10}$$

The plane stress anisotropic elastic stress-strain relation represented by engineering elastic constants is

$$\{\varepsilon_0\} = \begin{bmatrix} \frac{1}{E_{xx}} & \frac{-\nu_{yx}}{E_{xx}} & \frac{\eta_{xy,x}}{E_{xx}} \\ \frac{-\nu_{xy}}{E_{yy}} & \frac{1}{E_{yy}} & \frac{\eta_{xy,x}}{E_{yy}} \\ \frac{\eta_{x,xy}}{G_{xy}} & \frac{\eta_{y,xy}}{G_{xy}} & \frac{1}{G_{xy}} \end{bmatrix} \begin{Bmatrix} \sigma_x \\ \sigma_y \\ \tau_{xy} \end{Bmatrix} \tag{11}$$

where E_{xx}, E_{yy} are Young's moduli along x and y axes respectively; G_{xy} is shear modulus in xy plane; ν_{xy} and ν_{yx} are Poisson's ratios; $\eta_{xy,x}$,$\eta_{xy,y}$,$\eta_{x,xy}$,$\eta_{y,xy}$ are mutual influence coefficients; σ_x, σ_y and τ_{xy} are tensile stress along the x direction, tensile stress along the y direction and shear stress in the xy plane respectively.

By $N_x = h\,\sigma_x$, $N_y = h\sigma_y$, $N_{xy} = h\tau_{xy}$, the equation (11) is written as:

$$\{\varepsilon_0\} = [\mathbf{a}]\{\mathbf{N}\} \tag{12}$$

where the compliance matrix is

$$[\mathbf{a}] = \begin{bmatrix} \frac{1}{E_{xx}h} & \frac{-\nu_{yx}}{E_{xx}h} & \frac{\eta_{xy,x}}{E_{xx}h} \\ \frac{-\nu_{xy}}{E_{yy}h} & \frac{1}{E_{yy}h} & \frac{\eta_{xy,x}}{E_{yy}h} \\ \frac{\eta_{x,xy}}{G_{xy}h} & \frac{\eta_{y,xy}}{G_{xy}h} & \frac{1}{G_{xy}h} \end{bmatrix} \tag{13}$$

Comparing eqn. (13) with (10), it can be shown that

$$[\mathbf{a}] = [\bar{\mathbf{a}}] \tag{14}$$

From eqn. (14) the engineering elastic constants E_i, ν_{ij}, G_{ij} and η_{ij} may be determined using WFM (Woven Fabric Micromechanics).

FEM : The structure, in this case a cylindrical shell, is divided into number of small elements that are connected at the corners called nodes. One of such elements is shown in figures 8 and 9. At first, the displacements are determined using Rayleigh-Ritz technique, where a shape function is assumed for each component of displacement as given below:

$$\begin{aligned} \mathbf{u} &= \mathbf{a}_1 + \mathbf{a}_2\mathbf{x} + \mathbf{a}_3\mathbf{y} + \mathbf{a}_4\mathbf{xy} \\ \mathbf{v} &= \mathbf{b}_1 + \mathbf{b}_2\mathbf{x} + \mathbf{b}_3\mathbf{y} + \mathbf{b}_4\mathbf{xy} \\ \mathbf{w} &= \mathbf{c}_1 + \mathbf{c}_2\mathbf{x} + \mathbf{c}_3\mathbf{y} + \mathbf{c}_4\mathbf{x}^2 + \mathbf{c}_5\mathbf{xy} + \mathbf{c}_6\mathbf{y}^2 + \mathbf{c}_7\mathbf{x}^3 \\ &\quad + \mathbf{c}_8\mathbf{x}^2\mathbf{y} + \mathbf{c}_9\mathbf{xy}^3 + \mathbf{c}_{10}\mathbf{y}^2 + \mathbf{c}_{11}\mathbf{x}^3\mathbf{y} + \mathbf{c}_{12}\mathbf{xy}^3 \end{aligned} \tag{15}$$

where the constants a_1 to a_4, b_1 to b_4, and c_1 to c_{12} are expressed in terms of the nodal displacements and rotations:

$$\begin{aligned} \mathbf{u}_1 &= \mathbf{u}_{y=0}^{x=0} = \mathbf{a}_1 \\ \theta_{x_1} &= \frac{\partial \mathbf{w}}{\partial \mathbf{y}}^{x=0}_{y=0} = \mathbf{c}_3 \end{aligned} \tag{16}$$

The shape functions are substituted in the total potential expression,

$$\mathbf{U} + \mathbf{V} = \mathbf{f}(\mathbf{u}_1, \mathbf{v}_1, ...) \tag{17}$$

and then the principle of minimum total potential is applied to arrive at a system of equations for displacements.

Using Kirchoff-Love hypothesis, the laminate strains are evaluated as given below:

$$\varepsilon_x = \frac{\partial \mathbf{u}}{\partial \mathbf{x}}$$

$$\varepsilon_y = \frac{\partial u}{\partial y} + \frac{w}{r_y} \qquad (18)$$

$$\gamma_{xy} = \frac{\partial u}{\partial y} + \frac{\partial v}{\partial x}$$

where r_Y is the radius of the shell. By substitution of laminate strains in stress-strain relations the stresses in the coal support-bed are expressed as:

$$\begin{Bmatrix} \sigma_x \\ \sigma_y \\ \tau_{xy} \end{Bmatrix} = \begin{bmatrix} \overline{Q}_{11} & \overline{Q}_{12} & \overline{Q}_{16} \\ \overline{Q}_{12} & \overline{Q}_{22} & \overline{Q}_{26} \\ \overline{Q}_{16} & \overline{Q}_{26} & \overline{Q}_{66} \end{bmatrix} \begin{Bmatrix} \varepsilon_x \\ \varepsilon_y \\ \tau_{xy} \end{Bmatrix} \qquad (19)$$

where $[\overline{Q}]$ is a reduced stiffness matrix.

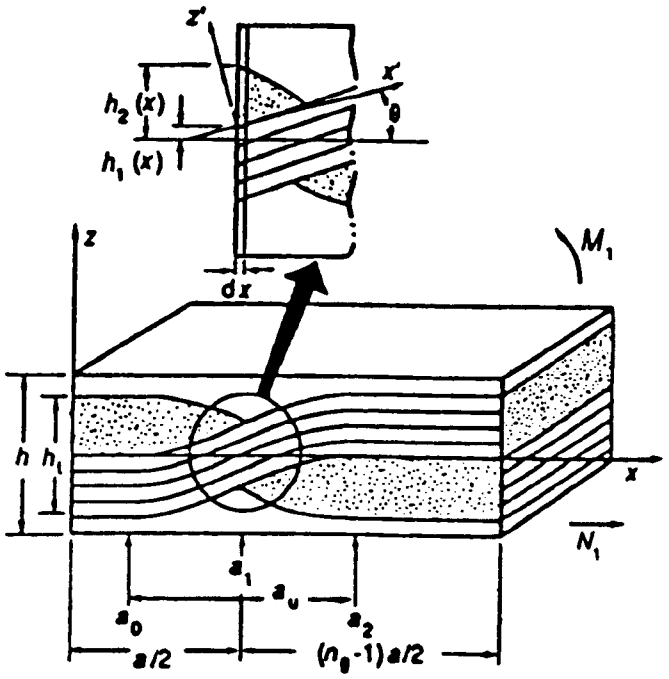

FIGURE 6: THE CRIMP (FIBER UNDULATION) MODEL

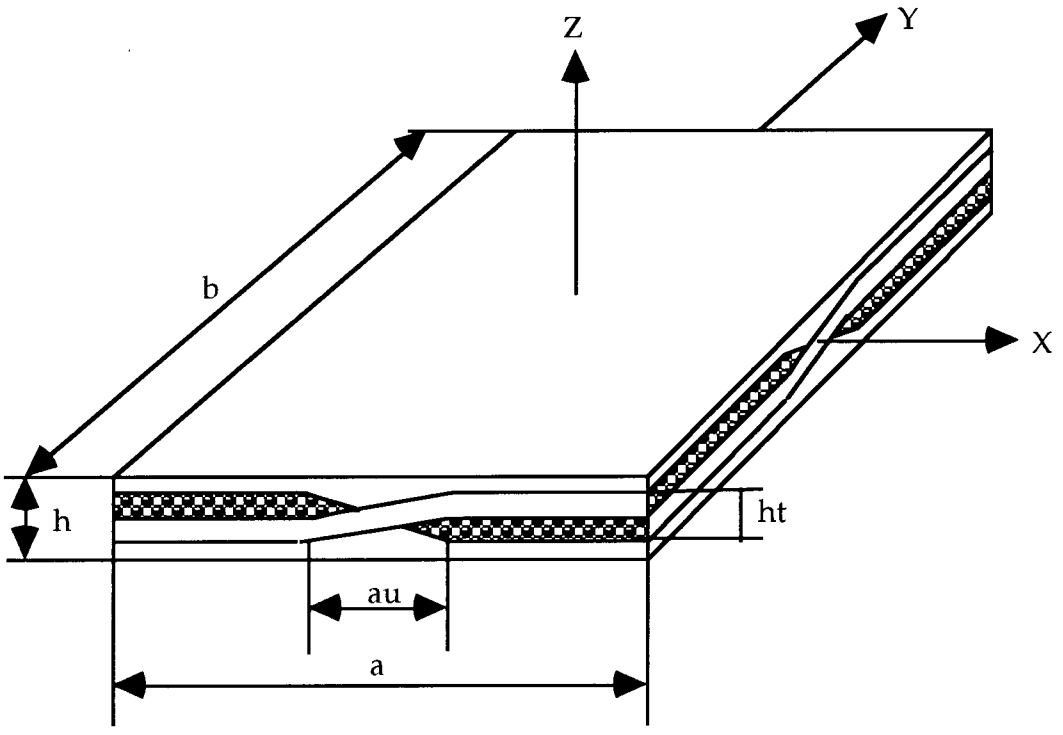

FIGURE 7: REPRESENTATIVE VOLUME ELEMENT

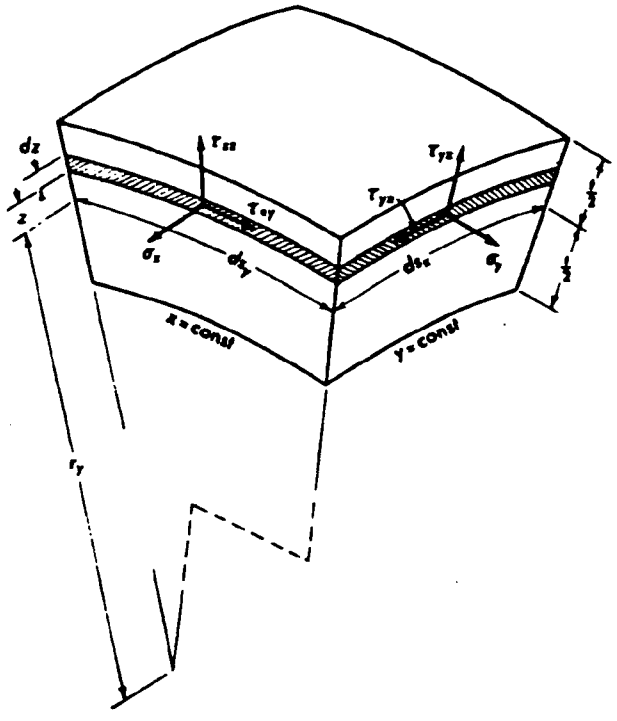

FIGURE 8: A SHELL ELEMENT

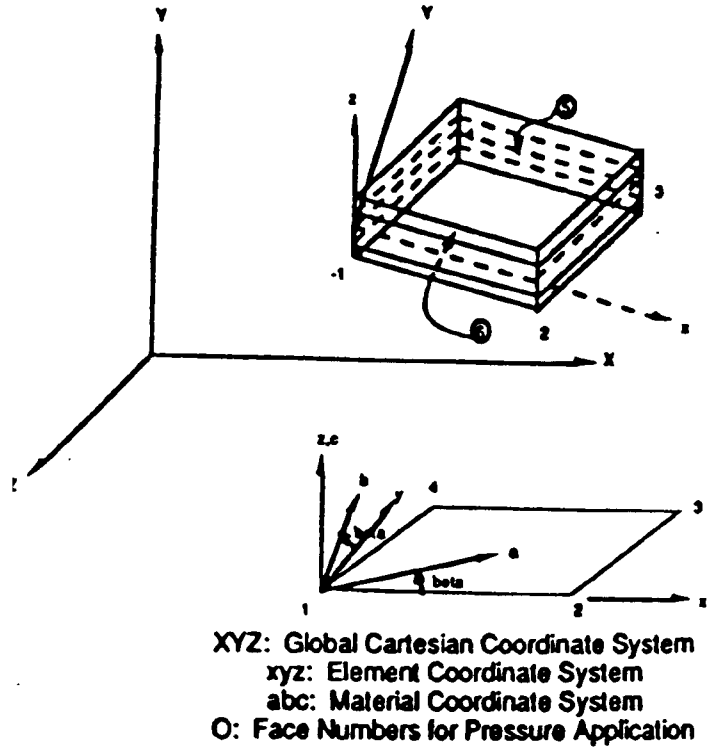

FIGURE 9: SHELL4L REPRESENTATION OF AN ELEMENT

2.2 Fabric Impregnation

Many techniques [9,10] are available for impregnating fabrics with resin matrix. The hand lay-up process is found to be inexpensive as well as the simplest of all [9]. The basis of this process is to spread the fabric over a mold and brush in the resin, which is room temperature curable. Care should be taken to ensure that the fabric is fully wetted out. The entrapped air is

squeezed out during the lay-up and skill is needed to avoid resin rich or resin starved areas. Tensioning a transparent membrane (for example a nylon sheet) over the impregnated fabric, before working out the excess resin and air, improves the quality of the fabric composite. The impregnated fabric is cured at room temperature for twenty-four to thirty-six hours depending upon the resin system used. At the end of this stage, gelation of the resin is complete and the fabric can be handled.

Another technique found to be suitable for fabricating thin section fabric composites is the Vacuum bag or Pressure bag technique [10]. This technique involves the application of a uniform pressure over the surface of the fabric impregnated with a resin. This is attained by producing a vacuum inside the bag in which the impregnated fabric is draped over.

2.3 Fabric Tensile Strength Characterization

High modulus fibers, used for reinforcement of thermoset or thermoplastic resin system, do not have unique tensile strengths. Flaws abound in these materials and hence the tensile strength of a given filament is a statistical variable. As the probability of finding severe flaws increases as length increases, mean tensile strength decreases with increasing gage length. This has been reported for several fibers including Kevlar 49 aramid (figure 10) [11]. Besides the change in the mean filament tensile strength with length, there is considerable scatter at a fixed length. Because of the statistical nature of filament strength, the failure of structures made from groups of fibers, such as yarns or strands or fabrics, are the end result of complex processes. The simplest multiple filament structure is an untwisted yarn,

which is a parallel-fiber bundle. Mean bundle strength is almost always less than that of the mean strength of the filaments of which it is composed.

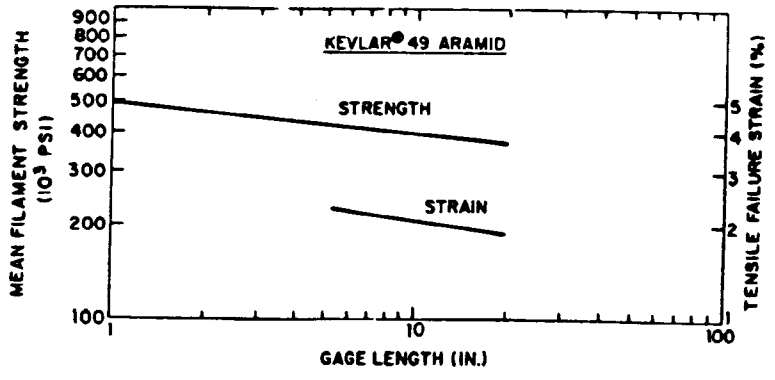

FIGURE 10: GAGE LENGTH EFFECT ON KEVLAR 49 FIBER

In Ref [12] this is explained with a simplistic model. As a bundle is loaded, filaments break randomly. When they do, the load they support is redistributed among the unbroken filaments, subjecting them to an increase in stress. Once filaments begin to break, the stress in the intact fibers is greater than average fiber stress, defined as load divided by total cross-sectional area. The bundle fails when the unbroken fibers cannot sustain an increase in load. Because of the failure process, in which scattered fiber breakage overloads the remaining fibers, the average stress at failure is less than that of the mean strength of filaments tested individually.

In the case of resin impregnated yarns or strands, that are composite materials, the failure process is complex. The matrix provides a mechanism for transmitting load from broken filaments to the intact filaments in the cross section. Several statistical theories that explain the complex failure process in unidirectional fibrous composites have been put forth [23-25], but not many in the case of resin impregnated fabric.

Considering the large dimension of the fabric replacing aluminum coal support-bed, and the statistical nature of the breaking strength of its constituent (fiber), a clear understanding of the failure phenomena in impregnated and unimpregnated fabric is essential. It is the objective of this experimental analysis to find if the resin impregnation stabilizes the tensile strength as this would enable acquiring a fabric of specific strength requirements.

2.4 Fatigue Life Prediction

During the life of composite structures, microevents generally occur which affect the strength and life of the structures. These events in their collective form are called damage. Whereas metals usually fail by crack initiation and growth in a manner which has come to be predictable through fracture mechanics analysis, composites exhibit several modes of damage including delamination, matrix crazing, fiber failure, void growth, matrix cracking, and composite cracking [13]. A particular structure may exhibit any or all of these damage modes, and it is difficult to predict which mode will dominate and cause failure.

In general fiber reinforced composites have a superior behavior when compared to metals, especially under tension-tension fatigue loading. However, fatigue failure has as well to be expected. In metals, the endurance limit is in the range of 40% of the static fracture stress, while in composites about 60-80% of the static fracture stress has to be reached in each consecutive load cycle before fatigue failure can occur [14]. However, the composite constituents (fiber, matrix, interphase) also influence fatigue behavior. The higher the Young's modulus of fibers, the lower the fatigue sensitivity [15]. But matrix properties can also have a positive effect on fatigue behavior; especially higher matrix fracture strains, which lead to an increase in fatigue life. In general unwoven materials are superior to woven materials in fatigue [13], as shown in figure 11.

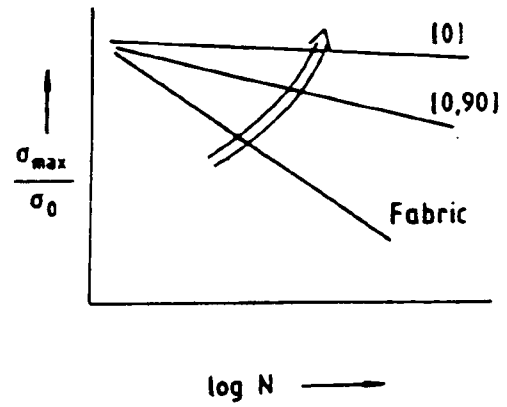

FIGURE 11: FATIGUE PERFORMANCE OF WOVEN AND UNWOVEN MATERIALS

The service life requirement of Gunderson, Inc., on the impregnated fabric replacing aluminum coal support-bed is ten years [25]. To avoid failure during this service period, it is necessary to understand, characterize, and model the life limiting process.

2.5 Chemical Resistance of Impregnated Fabric

One of the most common impurities in coal is sulphur, which is usually present in the volatile products and in the ash, and is derived chiefly from Iron Pyrites (Bi-Sulphide of Iron) in the coal. In addition, coal always contains a certain amount of water, the percentage depending on a great variety of circumstances. Wet coal yields sulfuric acid, which has been found to degrade the mechanical properties of Kevlar [16, 17]. At neutral pH (pH7), DuPont reports that the filament tenacity remains virtually unchanged after exposure at 149°F for more than 200 days. The further the pH deviates from pH7, the greater the loss in tenacity. Acidic conditions cause more severe degradation than basic conditions at pH levels equidistant from neutral.

In certain fluids the polyurethanes swell, but when removed and allowed to dry out they return to their original dimensions. This is not always so with other elastomers since they may contain plasticizers which can be leached out by the fluid, resulting in permanent shrinkage. The resistance of polyurethane elastomers to immersion in water has been identified as relatively poor and is directly applicable to immersion in dilute solutions of inorganic materials in water. Provided the inorganic substance has no catalytic effect the solution can be expected to behave as pure water.

However, acidic or alkaline media accelerate hydrolytic attack and therefore solutions of salts of weak acids or bases are likely to degrade polyurethanes faster than water. As a generalization it can be stated that provided the pH of a solution lies between the values of 5.5 and 8, the action of the solution can be considered similar to the action of water. At higher acidities or higher alkalinities it is advisable to test the effect of the particular solution.

This study aims at evaluating the performance of the impregnated fabric in solutions of different pH, in acidic solutions with increasing time, and in acidic solution at 212°F for ten hours to compare the performance of impregnated fabric with unimpregnated fabric in similar environment given in ref [17].

3. SOFTWARE, MATERIALS AND TESTING

3.1 Software

WFM : Woven Fabric Micromechanics (WFM), developed by University of Delaware, Center for Composite Materials, was used to predict the thermoelastic properties of orthogonal woven fabric composites. Hybrid fabric composites are not dealt in this software. The microstructural parameters used in the program input are composition of the weave, geometric parameters describing fiber architecture, and constituent properties of the resin and woven reinforcement. The program output consists of linear properties associated with two mutually perpendicular directions in the plane of the fabric reinforced composite. The user of this software can select any one of the three models namely the mosaic model, the crimp model and the bridging model to obtain the inplane thermoelastic properties. All these three models are based on the classical laminated plate theory.

COSMOS/M : The COSMOS/M is a finite element analysis program which is capable of performing linear/nonlinear static, linear/nonlinear dynamic, buckling, heat transfer, fluid flow and electromagnetic analyses on 1-D, 2-D and 3-D models. Several modules are available for pre- and post-processing the COSMOS/M finite element models. GEOSTAR is one such a module that functions as an interactive graphic pre- and post-processing module to the COSMOS/M finite element analysis system. It is an interactive 3D CAD_like geometric modeler, mesh generator, and finite element pre- and post-processor. The finite element analysis involves selecting element group, modeling the geometry of the structure, generating

surface and elements, incorporating the material properties, specifying the boundary conditions, and finally the load application. Subsequent to the analysis step, GEOSTAR's extended graphic post-processing capabilities can be used to perform an in-depth evaluation of the analysis results.

3.2 Materials

FABRIC : Plain woven fabrics, used for fabrication of test coupons, were obtained from Hi-Pro-Form Fabrics, Inc. and North American Textiles (represented as HPF and NAT respectively in the following sections). The weavers' specifications for HPF and NAT are style 745 and type #N281-60 respectively. Both the fabrics were scoured to promote adhesion of resin to the fibers. HPF is approximately three times heavier than NAT, weighing 14.5 ounce per square yard, and is also more finely woven than NAT. Hence, NAT is very easily wet by almost all resins with viscosity in the range 300 to 700 centipoise. The fabric count, which is the number of warp and fill yarns per square inch, is the same (17 by 17) for both the fabrics. However, the denier, which is weight in grams of 9000 meters of a yarn, varies; 1140 denier for NAT and 3000 denier for HPF.

RESIN : Epoxy and polyurethane based resin systems were the matrix materials used to impregnate the fabric. Epoxy resins are characterized by a three membered ring known as the epoxy, epoxide, oxirane or ethoxyline group. Commercial epoxy resins contain aliphatic, cycloaliphatic or aromatic backbones. Treatment with curing agents or hardeners gives insoluble and intractable thermoset polymers. High chemical and corrosion resistance, good mechanical and thermal properties, outstanding adhesion to various

substrates, low shrinkage upon cure are some of the characteristics of epoxy resins.

EA 9412 and Uralite 3177 were respectively, the epoxy and polyurethane based resin systems used. These have two parts; parts A and B. EA 9412 contains epoxy resins in part A and polyglycoldiamine in part B. Uralite 3177 contains urethane prepolymer (Diisocyanate and Silicon Dioxide as chief constituents) in part A and urethane curative (Ethyl glycols and mixed Aromatic Alkyl Esters as chief constituents) in part B. EA 9412 and Uralite 3177 were obtained from Dexter Hysol and Hexcel respectively.

Uralite 3177, which gets the most application because of its better abrasion and wear resistance, and resilience than EA 9412, is a white casting polyurethane elastomer. The viscosity of the mixed resin system is 250 centipoise. To reduce the viscosity further and hence improve the flow of resin into finely woven fabric (HPF), Xylene was added to the resin mixture. The gelation of the mixed Uralite 3177 without the addition of Xylene takes twenty-four minutes, and with the addition of Xylene takes more than forty minutes. The complete cure, in both the cases, takes two to four days at room temperature.

3.3 Testing

TENSILE TESTING : The guidelines given under ASTM standards D3039 [18] were followed in determining the tensile strength of both epoxy and polyurethane impregnated fabrics. When using adapter grips, which were designed and fabricated specially for this study, a slight modification in

the coupon geometry, explained in the following paragraphs, was made. A brief explanation of the procedure involved in this test is given below:

The microcomputer controlled Instron 4505 (refer figure 12) used for tensile testing of fabric coupons consists of a stationary and a movable head. The crosshead speed is controlled by the computer to provide a nearly constant strain rate. A nominal value of 0.2 inch per minute was the strain rate used as it causes failure of the test coupons within one to ten minutes [18].

Test coupons varied in the gagelength. However, the width of the test coupons was almost the same for all test coupons, measuring approximately one inch. The thickness and the width of the coupons were measured at three locations along the gage length using a vernier caliper. The minimum area, minimum width multiplied by thickness, was recorded as the cross-sectional area for the test coupon.

Tabs of dimensions one inch width by two and a quarter inch length were used when testing unimpregnated fabric coupons for tensile strength. Tabs were not used for impregnated fabric. Two different grips, a wedge grip (refer figure 13) and an adapter grip (refer figure 16) were used. Manual force was applied for securing the coupons between the grips in the case of wedge grips obtained from Instron. Adapter grip, developed for this study, essentially consists of a hollow cylindrical steel block with slot for insertion of a pin and the fabric coupon. The geometry of the fabric coupons tested with adapter grips varies from that of the coupons tested with wedge grips. Adapter grip coupons have three regions namely the loop, the overlap, and

FIGURE 12: PHOTO OF INSTRON 4505, AND TENSILE TEST SET-UP

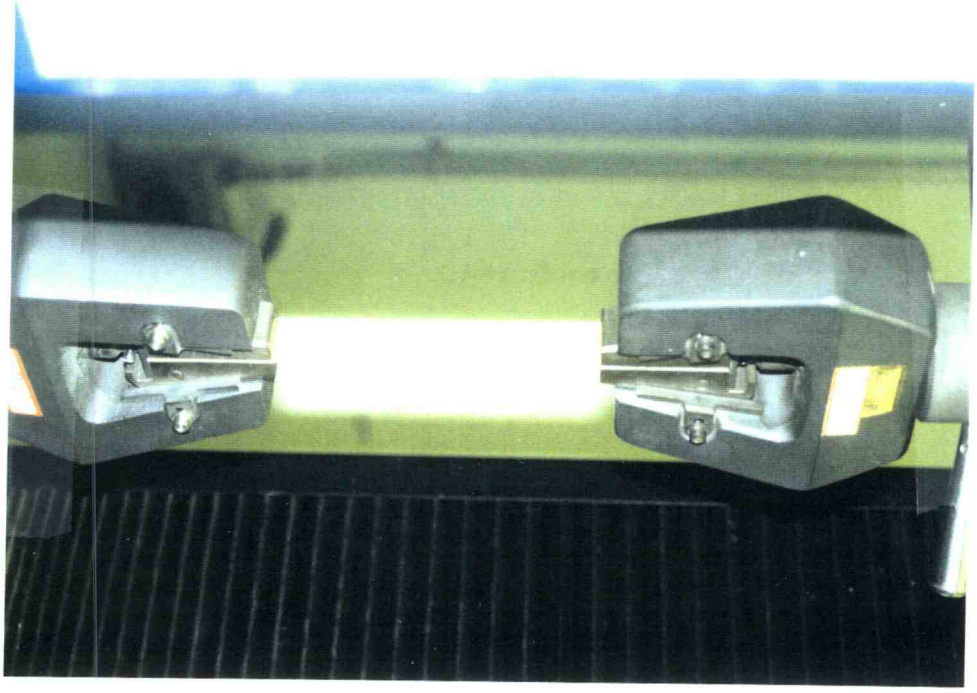

FIGURE 13: PHOTO OF WEDGE GRIPS, AND GRIPPING ARRANGEMENT

the gage length regions as shown in figure 14. Delamination arresters, basically two aluminum plates with bolts and nuts for tightening the plates, were used in the overlap region to promote failure in the gage section and prevent delamination in the overlap region.

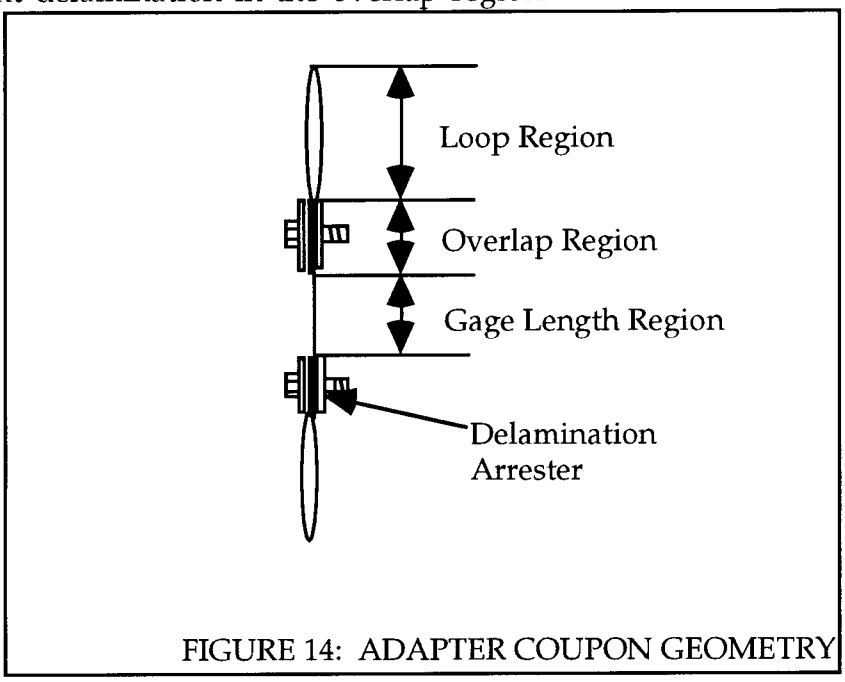

FIGURE 14: ADAPTER COUPON GEOMETRY

The density of the fabric composite samples, from the same panel where the coupons had been cut, was determined as per ASTM Standard D 792 [19]. This value was used for determining the void content as per Test Method B of ASTM Standard D 2734 [20]. The volume fraction of the fabric was determined using the following expression:

$$V_f = [(W_f/\delta_f) / (W_c/\delta_c)] \times 100$$

where:

W_f = weight of fiber in the composite,

W_c = weight of the initial composite specimen,

δ_f = fiber density,

δ_c = composite density.

Values obtained for volume fraction of fabric and void, from the above procedures, were used in the following expression for finding resin content, V_r, of the composite.

$$V_r = 100 - (V_f + V_v)$$

The test coupons were conditioned for twenty-four hours at 74 ± 2° F and a relative humidity of 50%. At least five coupons were tested per condition. Mean, standard deviation and coefficient of variation in percent, for fracture strength of the test coupons, were determined (Table 5).

FATIGUE TESTING : MTS Series 812(refer figure 16), a servo-hydraulic controlled testing machine, was used for testing both impregnated and unimpregnated fabric coupons. Fatigue tests were performed in load control using a sinusoidal waveform. Method A of ASTM Standards D 3479 [21] was followed in finding the fatigue life of the fabric coupons. The procedure is briefly explained below:

The average fracture strength of the coupons was used as the 100% level for the fatigue tests. The MTS Serial 812 machine was calibrated for load at 10% of its total load capacity and the calibration factor was found to be 221 pounds per volt. The voltage signal corresponding to the load acting on the coupons was monitored with the help of cathode ray oscilloscope (CRO). The CRO output was also checked with a hand-held digital multimeter. The test coupon was cycled between two tensile loads at 25 HZ frequency as recommended by Gunderson, Inc. The stress ratio, R, which is the ratio of minimum stress to the maximum stress was chosen arbitrarily. The value of R was 0.6 for NAT test coupons and 0.8 for HPF test coupons. After testing had begun, the loading was frequently checked and corrected.

The cycle counter was started when the coupon was subjected to fatigue load. Three multipliers, X1, X10, and X100 are available for counting

the number of cycles. The counter turns once at the completion of one cycle if coupled with X1 multiplier, turns once at the completion of ten cycles if coupled with X10 multiplier, and so forth. Because of the improper functioning of X10 and X100 multipliers, X1 had to be used and hence the fatigue test was run intermittently. However, the MTS machine is equipped with the facility of stopping the counter at the point of coupon failure.

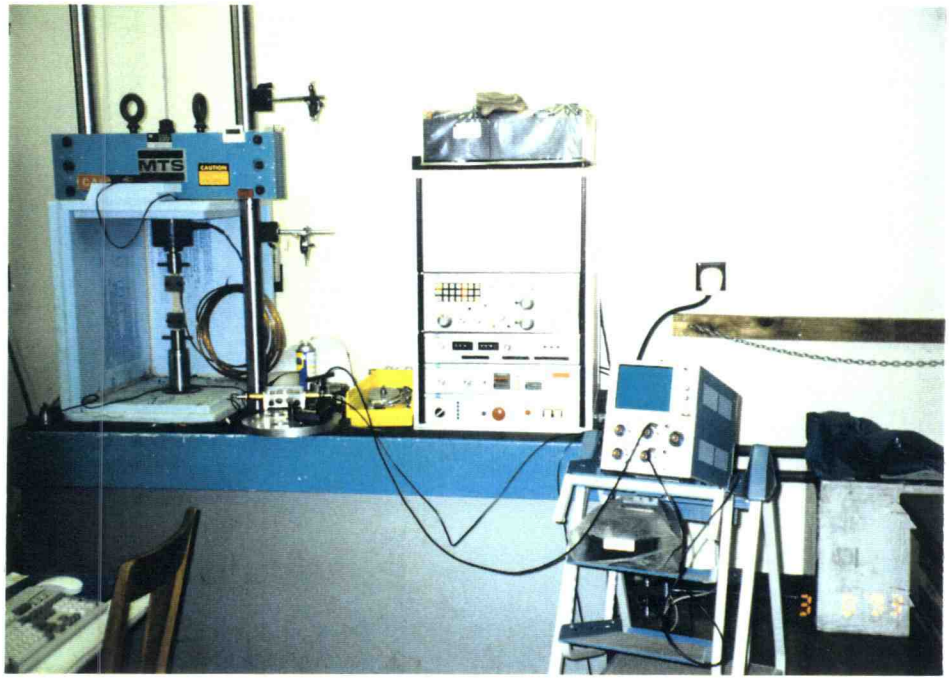

FIGURE 15: PHOTO OF MTS, AND FATIGUE SET-UP

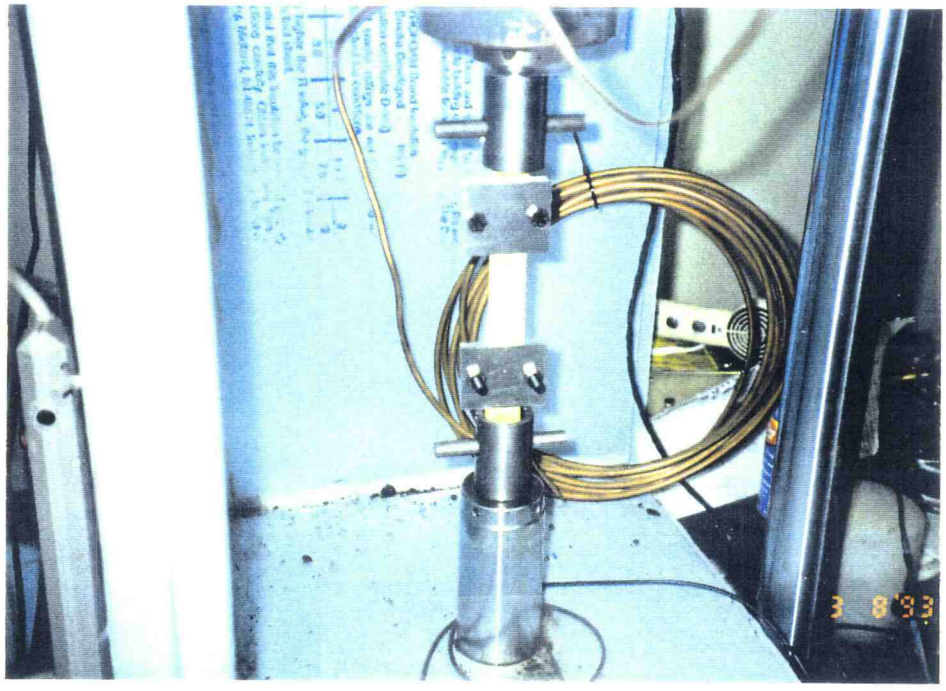

FIGURE 16: PHOTO OF ADAPTER GRIPS AND DELAMINATION ARRESTERS

4. APPROACH

4.1 Analytical Procedure for Stress Analysis

The maximum stresses, developed due to the pressure exerted by the coal in the railcar coal support-bed, were determined using WFM micromechanics and COSMOS finite element models. Two material systems, epoxy impregnated Aramid 29 fabric and epoxy impregnated Kevlar 49 fabric, were analyzed. A brief explanation of the procedure involved in this analysis is given below:

WFM : The crimp model calculations given in WFM were used for obtaining the elastic properties of impregnated fabric. The input for WFM includes the properties of a lamina; resin impregnated yarn, the properties of the resin used for impregnating the fabric, and the geometry of the fabric. A brief explanation of the input data for WFM is given below:

Lamina and Resin Properties : The resin impregnated yarn properties (table 1) for Kevlar 49/epoxy and Aramid 29/epoxy were excerpted from references 17 and 22. Because the mechanical properties of polyurethane resin were not available in many literature reviewed [27-29], the resin impregnated in the Kevlar 49 and Aramid 29 yarns was assumed to be epoxy. The properties of polyurethane resin (two component casting elastomer) need to be experimentally determined. The volume fraction of fibers in both Kevlar 49/epoxy and Aramid 29/epoxide was sixty percent. The values for Poisson's ratios; NU_{12} and NU_{23}, and coefficients of thermal expansion; AL_1 and AL_2 were assumed to be similar to those of graphite/epoxy. Although this approach might not yield exact properties of polyurethane impregnated

TABLE 1: WFM INPUT

Detail	Parameters	Values	Unit
Geometrical Input	n_g	2	....
	h	0.028	in.
	h_t	0.025	in.
	a	0.059	in.
	a_u	0.055	in.
Lamina Properties Aramid 29/Epoxide V_f = 60%	E_1	7.2548E+06	lb./ in.^{2}
	E_2	0.72548E+06	lb./ in.^{2}
	G_{12}	0.43529E+06	lb./ in.^{2}
	NU_{12}	0.222	....
	NU_{23}	0.25	....
	AL_1	-0.222E-05	in./in.°F
	AL_2	0.439E-04	in./in.°F
Lamina Properties Kevlar 49/Epoxy V_f = 60%	E_1	0.11E+08	lb./ in.^{2}
	E_2	0.80E+06	lb./ in.^{2}
	G_{12}	0.33E+06	lb./ in.^{2}
	NU_{12}	0.340	....
	NU_{23}	0.380	....
	AL_1	-0.222E-05	in./in.°F
	AL_2	0.439E-04	in./in.°F
Matrix Properties Epoxy	E_M	0.499E+06	lb./ in.^{2}
	G_M	0.185E+06	lb./ in.^{2}
	NU_M	0.350E+00	....
	AL_M	0.320E-04	in./in.°F

Kevlar 29 fabric, it would help in predicting the strength requirements on the impregnated fabric. This analysis would also inform basic difference in the impregnated Kevlar 49 and Aramid 29 fabric as the railcar bed.

Fabric Geometry : The pattern of repeat of interlaced regions is denoted in WFM by a geometrical parameter n_g. The value of n_g for a plainweave is two. The parameter h_t corresponds to the thickness of Kevlar 29 fabric bought from Hi-Pro-Form Fabrics, Inc. (HPF has higher strength than NAT from weavers' data sheet). As there are seventeen yarns per inch of this fabric, yarn width a is equal to one seventeenth of an inch. Values for other parameters, the thickness (h) and the length of undulated region (a_u) were assumed to be 0.028 and 0.055 inches respectively.

COSMOS : The basic information needed for the design of the railcar floor was furnished by Gunderson Inc., Portland, OR. This information is provided in table 2. The element group shell4l, which considers a four-node

TABLE 2: DESIGN REQUIREMENTS

Sl. No.	Requirements
1.	Vertical load should be designed for 1.8 load factor.
2.	Design should incorporate 0.45g lateral acceleration.
3.	Design should also consider 2g impact.
4.	Railcar should be designed to carry 240,000 pounds of coal.

multilayer quadrilateral shell element with bending and membrane capabilities for analysis, was chosen to represent the coal-support-bed. The

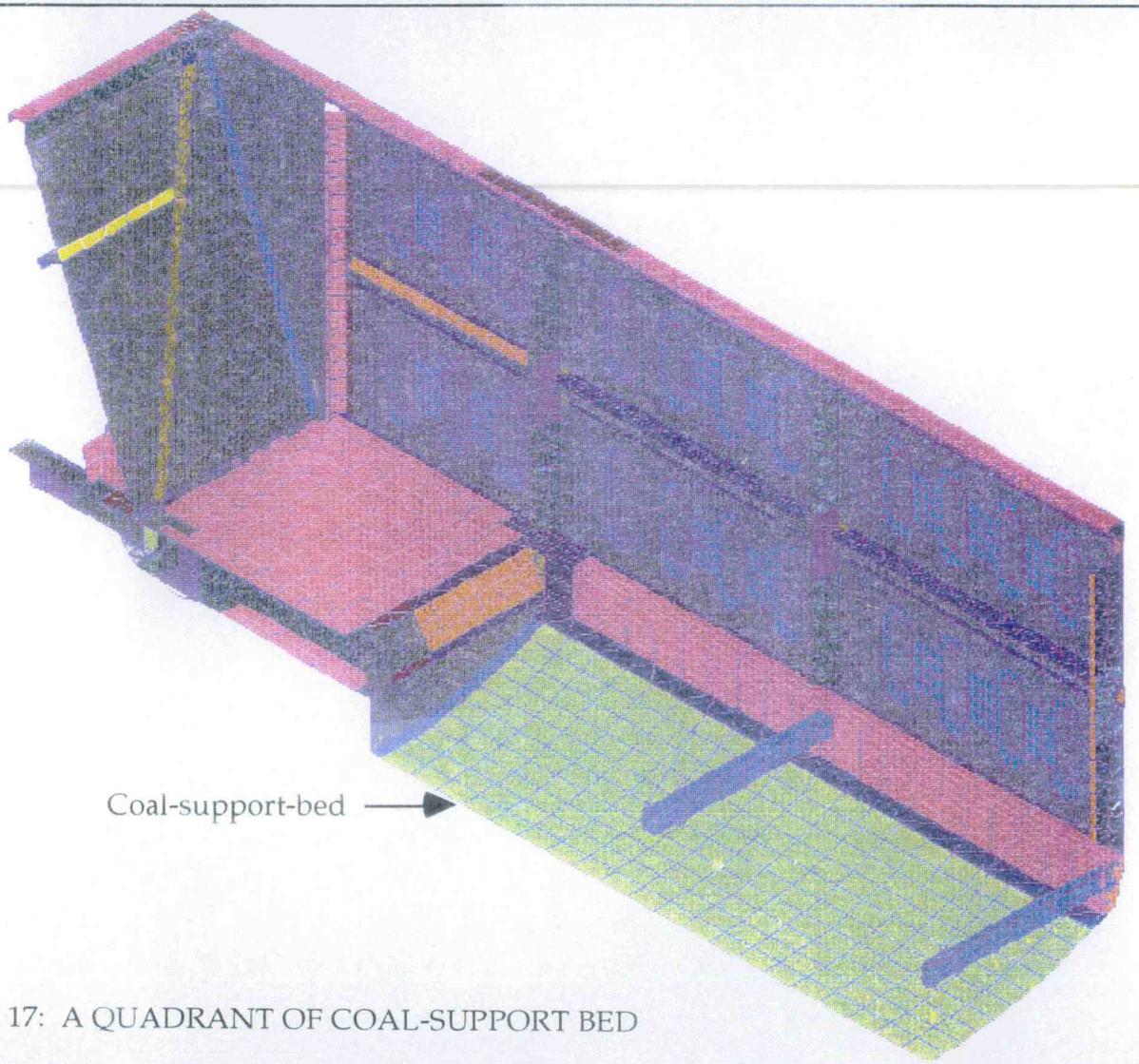

FIGURE 17: A QUADRANT OF COAL-SUPPORT BED

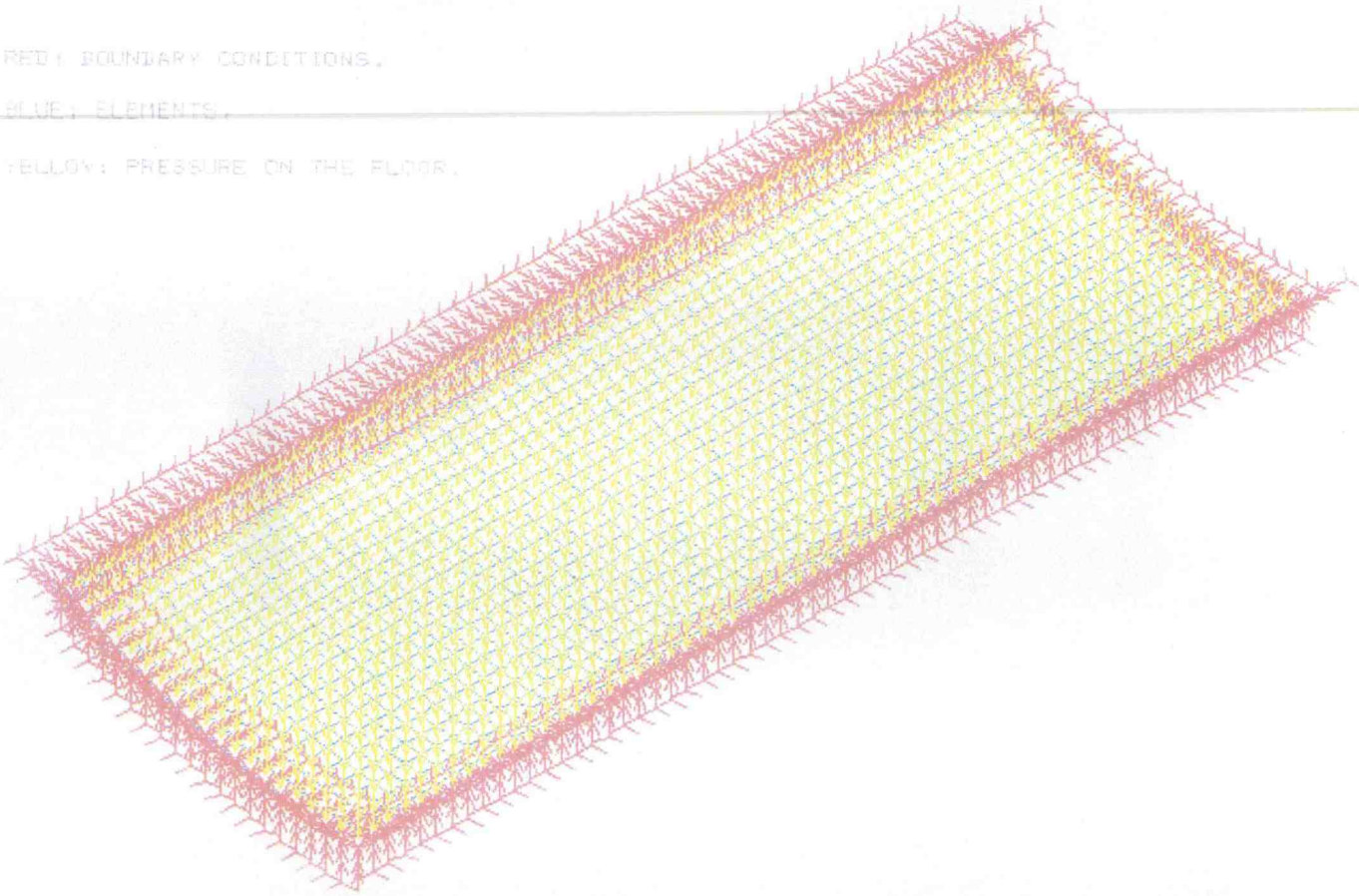

FIGURE 18: FEM MODEL SHOWING BED, BOUNDARY CONDITIONS AND LOADIND.

TABLE 3: COSMOS INPUT

Detail	Parameters	Values	Unit
Geometrical Input	Length of the floor	360	in.
	Width of the floor	119.93	in.
	Radius r_y	120	in.
	Thickness t	0.028	in.
Fabric Properties Aramid 29/Epoxy	E_x	0.170E+07	lb./ in.^{2}
	E_y	0.949E+06	lb./ in.^{2}
	G_{xy}	0.363E+06	lb./ in.^{2}
	NU_{xy}	0.679E-01	....
Fabric Properties Kevlar 49/Epoxy	E_x	0.179E+07	lb./ in.^{2}
	E_y	0.113E+07	lb./ in.^{2}
	G_{xy}	0.29E+06	lb./ in.^{2}
	NU_{xy}	0.763E-01	....
Load on the floor	Static Pressure + Lateral accn.	11.118	lb./ in.^{2}

material properties obtained from WFM (fabric properties in table 3) were used as COSMOS input (table 3). A single layer of impregnated fabric wasused as a model for the coal support-bed. Due to symmetry of the geometry and material properties, only a quadrant of the coal support-bed (figure 17) was analyzed. Elements of area approximately equal to one square inch were created and all the four sides of the floor were clamped as shown in figure 18.

Since the lateral acceleration or the centrifugal force is exerted on the side walls of the railcar, only impact and static loads are considered in determining the pressure acting on the coal support-bed. The maximum impact load, experienced by the bed on loading coal, is calculated as given below:

$$\text{Load due to impact of coal} = 2g \times \text{Mass of coal}$$
$$= 480{,}000 \text{ lb.}$$

The static load on the coal support-bed, which is designed for a factor of safety 1.8, is 432,000 lb.. This load is less than the load due to impact of coal on the bed. Hence the impact load is considered in determining the pressure acting on the coal support-bed.

$$\text{Pressure acting on the car bed} = \frac{\text{Total Load}}{\text{Floor Area}}$$
$$= \frac{540{,}000}{360 \times 119.93}$$
$$= 11.118 \text{ lb./ in.}^2.$$

4.2 Impregnation Procedure

Hand lay-up and vacuum-bag techniques were used in impregnating HPF and NAT fabrics. NAT fabric was very coarsely woven and scoured, therefore fabric wettability was not a problem. On the contrary, HPF was very finely woven. Despite the scouring of the fabric, problem was faced in completely wetting the fabric. Hence efforts were made in decreasing the viscosity of Uralite 3177 by heating the resin components, and adding Xylene. Seven different procedures, based on the resin application on the fabric, heating and addition of xylene, and impregnation technique, were adopted to make fabric samples. The test coupons, cut from these samples, were statically tested in the Instron 4505 for tensile strength. This was done to find out the optimum procedure that provides the best fabric wettability, least void, and high strength in the fabric composite.

Seven fabric samples, each of dimensions six inches (fill direction) by fifteen inches (warp direction), were cut from the fabric bundle obtained from Hi-Pro-Form Fabrics, Inc. (HPF). A special purpose scissors, obtained from Wolff Industries, Inc., was used to cut the fabric. The lower blade of this pair of scissors had been corrugated to hold the fabric from sliding and the top blade was razor edged to cut even the most finely woven fabrics. Uralite 3177, a polyurethane resin system, was used for impregnating the fabric. Equal weights of the two parts of the resin system were mixed thoroughly using a stirrer. Batch 1 through Batch 5, and Batch 7 samples were fabricated using hand lay-up technique while Batch 6 sample using vacuum bag technique.

The basic procedures for the impregnation of test coupons are explained below:

HAND LAY-UP: The sample was spread over a nylon sheet and was painted with the polyurethane resin mixture using an ordinary paint brush. Another nylon sheet was stretched over the painted fabric. A steel spindle was then rolled over this set-up (figure 19) for removing excess resin and entrapped air-bubbles. The pressing of the painted fabric also helps obtaining an almost uniform thickness over the entire impregnated area. The painted fabric was cured at room conditions for two to four days. The painted fabric, left on the nylon sheet itself, had a rough bottom surface after curing. Therefore it was removed from the nylon sheets and hung in the air to cure at room conditions.

VACUUM-BAG: Two nylon sheets larger than the sample to be impregnated were cut. The vacuum bag sealant, was laid on one of the sheets as shown in figures 20 and 21. One end of a tube was connected to a vacuum pump and the other end was firmly placed on the sealant. The end of the tube inserted into the bag was tied with a filter cloth (dust mask material) to prevent the flow of excess resin through the tube to the vacuum pump. Bleeder cloth, which absorbs excess resin and facilitates exit of entrapped air through the tube, was placed on the nylon sheet. A perforated release film was used between the fabric and bleeder cloth to prevent the sticking of fabric and bleeder cloth. The pores in the release film facilitate flow of entrapped air-bubbles. Another set of perforated release film and bleeder cloth was spread over the impregnated fabric. The bag was then sealed so that it was air-tight. Besides the atmospheric pressure, hand pressure was applied on the bag using a steel spindle to facilitate the removal of excess resin and air-bubbles.

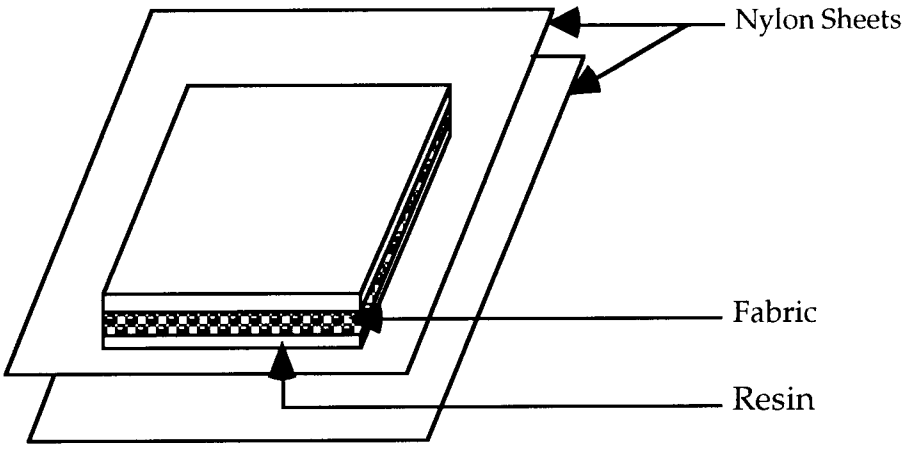

FIGURE 19: HAND LAY-UP SET-UP

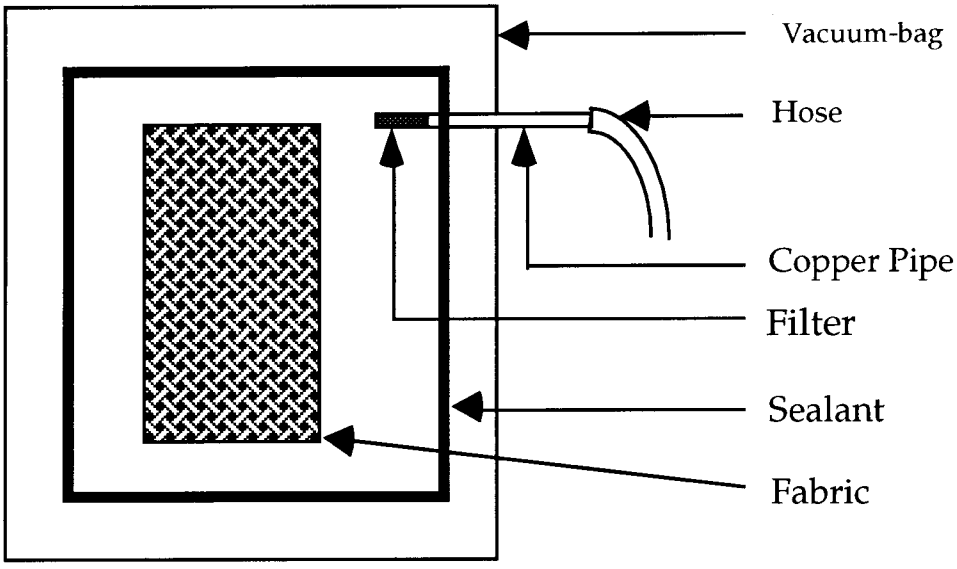

FIGURE 20: PLAN VIEW OF VACUUM-BAG FABRICATION SET-UP

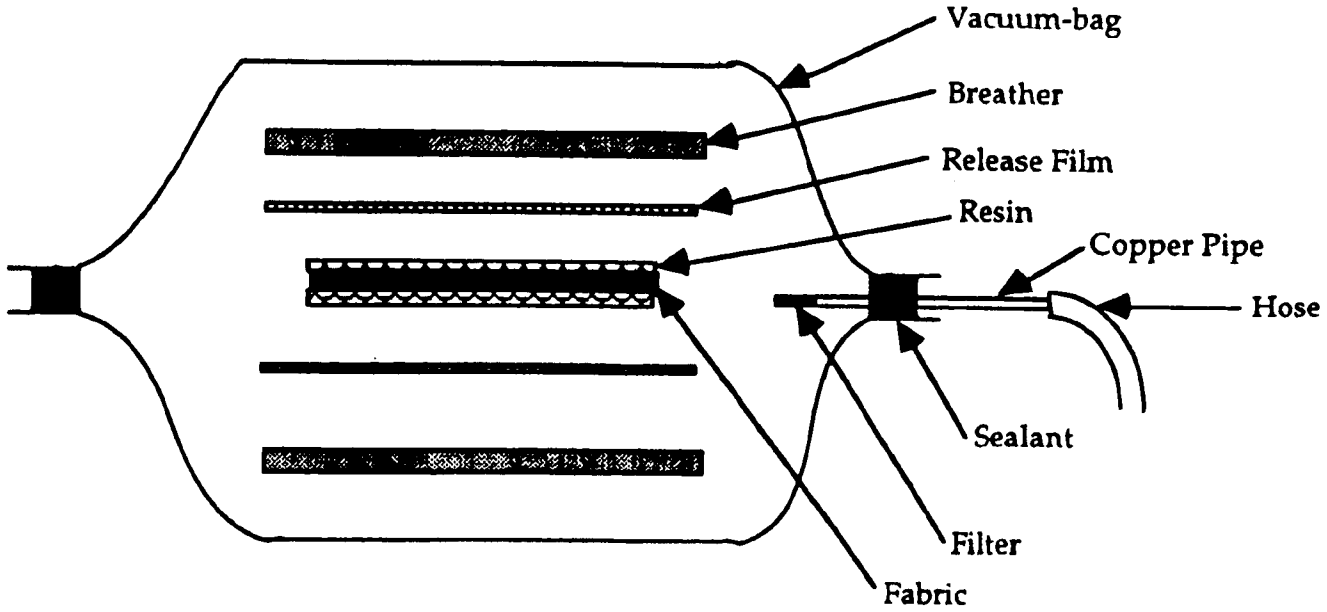

FIGURE 21: SIDE-VIEW OF VACUUM-BAG FABRICATION SET-UP

In all these techniques the weight of the fabric before and after coating was measured and used to determine the volume fraction of the fabric, the resin and the voids in the fabric composite. Steps involved in the seven different procedures adopted for impregnating the test coupons, using these techniques are discussed below:

Batch 1 : Part A and part B of EA 9412 were mixed in 100:17 ratio whereas Equal weights of part A and part B of Uralite 3177 were mixed together thoroughly and the mixture was brushed on the top and bottom of the fabric specimen. The impregnated fabric was placed between two nylon sheets and then rolled over using a smooth steel spindle. This method was sufficient for impregnating NAT with either Uralite 3177 or EA 9412.

Batch 2 : The fabrication procedures are almost similar to those used for Batch 1 specimen preparation except that the resin mixture was brushed on only the top surface of the fabric instead of both the surfaces.

Batch 3 : One part of Xylene [$C_6H_4(CH_3)_2$] was added to six parts of the resin mixture on a volume basis. This mixture was then brushed only on the top surface of the fabric and then rolled over.

Batch 4 : Before painting on the fabric, Part A and Part B of Uralite 3177 were heated separately to 110-120° F for ten minutes in an oven.

Batch 5 : Equal weights of the constituents of the resin system were heated separately in an oven to 110-120°F for ten minutes. Xylene and resin mixture were added in 1:6 ratio respectively. All these components were stirred for two to three minutes. This mixture is workable for a relatively short time (less than twenty minutes). Therefore careful planning of the operation is necessary.

Batch 6 : Equal weights of part A and part B were mixed together and then brushed on the fabric. The impregnated fabric was placed in the vacuum bag and allowed to cure in the bag for two to four days.

Batch 7: The resin components were mixed thoroughly and painted on both the sides of the fabric sample draped over a nylon sheet. The painted fabric was not squeezed with the spindle in this procedure. The sample was left on the nylon sheet for cure. This procedure was adopted for only NAT as it is a coarsely-woven weave. The cross-sections of Batch 3 and Batch 5 samples, which had better strength than the other samples, were further analyzed on a microscopic level to observe void and resin distribution in the fiber bundles of the yarns.

4.3 Microstructure Analysis

The microstructure of the cross-sections along lines AA and BB(refer figure 22) was analyzed for Batch 3 and Batch 5 specimens. Cross-section AA has both warp and fill or weft yarns, whereas cross-section BB has only warp yarn. So cross-section BB must have more resin content than cross-section AA. The entrapped air-bubbles, if there were any, must be embedded in the resin. So different void distributions can be anticipated in these cross-sections. This examination was undertaken to know the extent of fabric wetting by the resin, volume content of pores in the representative area, and the essential difference in the microstructure between Batch 3 and Batch 5 specimens, as well as in the resin and void distribution between the cross-sections AA and BB. An understanding of this difference in the

microstructure would shed light on the effect of fabrication variables on the fracture strength of the impregnated fabric.

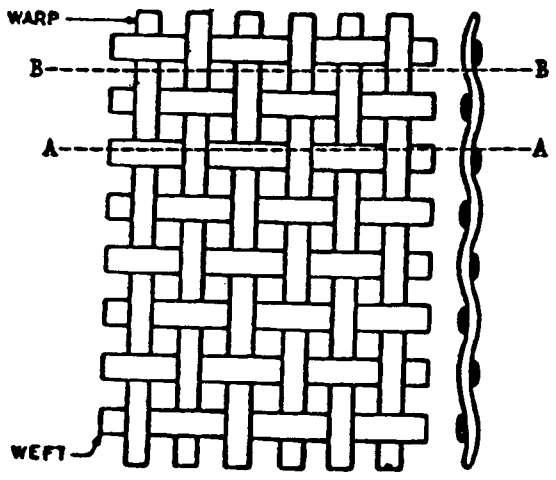

FIGURE 22: CROSS-SECTIONS OBSERVED UNDER OPTICAL MICROSCOPE

The specimens for microstructure analysis were coated on both sides with alumina powder. This prevented the disturbance of the fiber during polishing stages and also improved the contrast between the specimen and the mount, which have similar color, on the microphotograph. The coating mixture comprises of Xylene, Alumina powder (0.5 microns), and Uralite 3177 resin mixture in 1:3:6 ratio respectively. This resin mixture was painted on both the surfaces. The thickness of each coating was approximately 20 mils. The coating was allowed to cure at room temperature for two to four days.

Four strips, each of approximate dimensions 3/4 inch (fill direction) by 3/4 inch (warp direction) were cut using the special purpose scissors discussed earlier. Two of the strips were cut along line AA and the other two along

line BB. The strips were bundled together using a cellophane tape. This bundle was placed face down in the mold cup.

The specimen bundle (figure 23) was encapsulated in a mount, using the mounting system, Formula 1, obtained from Metallurgical Supply Company, Inc.. The specimen was polished in three stages: lapping stage, rough polishing stage, and final polishing stage. In the lapping stage, the specimen was lapped on 240, 320, 400, and 600 grit abrasive papers sequentially making sure the water was flowing uniformly over the abrasives. Before introducing it to the second stage of polishing, the specimen was cleaned in Methanol using an ultrasonic cleaner. Rough polishing of the specimen was done on revolving wheels using an abrasive slurry consisting of alumina powder in a water suspension. The alumina particle size for the initial rough polishing was five micrometers and that for the final rough polishing was 0.3 micrometer. The third and the final stage was also done on the revolving wheel but using 0.03 micrometer alumina abrasive powder in a water suspension. At this point the specimen was very smooth to the eyes, therefore ready for optical microscopic examination.

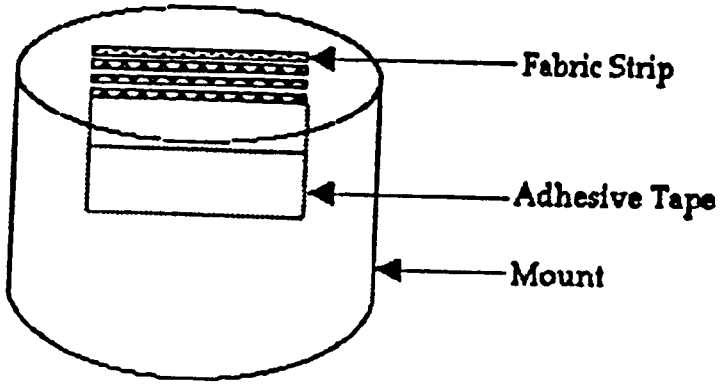

FIGURE 23: SCHEMATIC REPRESENTATION OF MICROSTRUCTURE SPECIMEN

4.4 Tensile Strength Characterization

The gage length effect behavior of unimpregnated HPF coupons of increasing gage lengths was characterized by loading the coupons monotonically in Instron 4505 using the wedge grips. The impregnated fabric coupons were made as per the procedure adopted for impregnating Batch 1 and Batch 3 samples. Uralite 3177 was used in the impregnated HPF samples. The objective behind using impregnated and unimpregnated, and Batch 1-type and Batch 3-Type samples is to analyze the effect of resin impregnation and varying fabrication procedure on the gage length effect behavior of the fabric. The results are given in section 5.2.

Test coupons, for gage length behavior study, were also made from NAT fabric. Resins used for impregnating NAT fabric were EA 9412 and Uralite 3177. Because of the coarseness of weaving and good fabric wettability in NAT, no extra effort was spent in decreasing the viscosity of the resin mixture. Hence Uralite impregnated NAT coupons were made as per Batch 1 fabrication procedure and EA 9412 impregnated coupons by mixing part A and part B in 100:17 ratio on a weight basis. The coupons were tested statically for tensile strength using both wedge and adapter grips. These tests, basically intended for observing and analyzing the gage length behavior, would also provide valuable information (section 5.3) on the effect of different weaves, resins and grips on the strength characteristics of the impregnated fabric.

4.5 Fatigue Test Approach

Fatigue tests were done on unimpregnated, Batch 5-type and Batch 6-type HPF coupons using wedge grips in MTS testing machine. Batch 7-type NAT coupons were also tested for fatigue life, but using adapter grips. Gage lengths of unimpregnated HPF coupons, impregnated HPF coupons, and impregnated NAT coupons were five and ten inches, ten inches, and 5 inches respectively.

4.6 Chemical Resistance Test Procedure

Batch 5-type test coupons were used for this study. The weight of the coupons was measured before soaking them in solutions of pH 2, 5, and 10. These were prepared by mixing sulfuric acid with distilled water for pH 2 and 5, and ammonium hydroxide with distilled water for a pH of 10. Ten percent concentrated sulfuric acid solution was prepared by mixing sulfuric acid with distilled water in 1:10 proportion on a volume basis. Five coupons were soaked in each of these solutions. The tray, containing the coupons in the solution, was covered to prevent evaporation of vapor. The effect of acidic solution at elevated temperature, and two other variables (given below) on the tensile strength of impregnated HPF coupons were studied. They were:

1. The effect of solutions of different pH : In this case, the trays containing the test coupons in the solutions of pH 2, 5, and 10 were kept in an oven at 122° F for seventy-five hours. The pH of the solution was monitored regularly and kept constant throughout this duration.

2. The effect of time : In this case, the trays containing the test coupons in a solution of pH 2, were kept in the oven at 122° F for 30, 75 and 115 hours.

3. The effect of acidic solution at elevated temperature : The test coupons in a ten percent concentrated sulfuric acid solution were kept in the oven at 212 ° F for ten hours.

After taking out of the oven, the coupons were wiped and allowed to dry for fifteen minutes at room conditions. The weight of samples were measured to determine the moisture absorption by the coupons. The coupons were then tested for tensile strength in Instron 4505.

5. RESULTS AND DISCUSSIONS

5.1 Stress Analysis of Coal-Support-Bed

Table 4, and figures 24 and 25 , the results of FEM analysis, show the maximum in-plane stresses, Sigma X and SigmaY, and the Z-direction displacement due to the load acting on the coal-support-bed. In this analysis, Sigma X and Sigma Y can be interpreted as the stresses acting in the lengthwise (Warp direction) and widthwise direction (Fill direction) of the coal-car respectively. When the fabric properties were input to COSMOS, care was taken to align the warp-direction properties with the X-direction of the elements (refer figure 5 for element and material directions) generated in the software.

TABLE 4: MAXIMUM STRESSES AND DISPLACEMENTS IN THE COAL-SUPPORT-BED

Coal-Support-Bed Material	Maximum Stress [lb./in.^{2}]		Displacement in Z Direction [in.]
	Sigma X	Sigma Y	
Aramid 29/ Epoxy	53,800	12,200	9.47
Kevlar 49/ Epoxy	53,700	12,400	7.95

For Aramid 29/Epoxy as the coal-support-bed, this analysis predicts a maximum Sigma X of 53,800 pounds per square inch at the bottom of the bed,

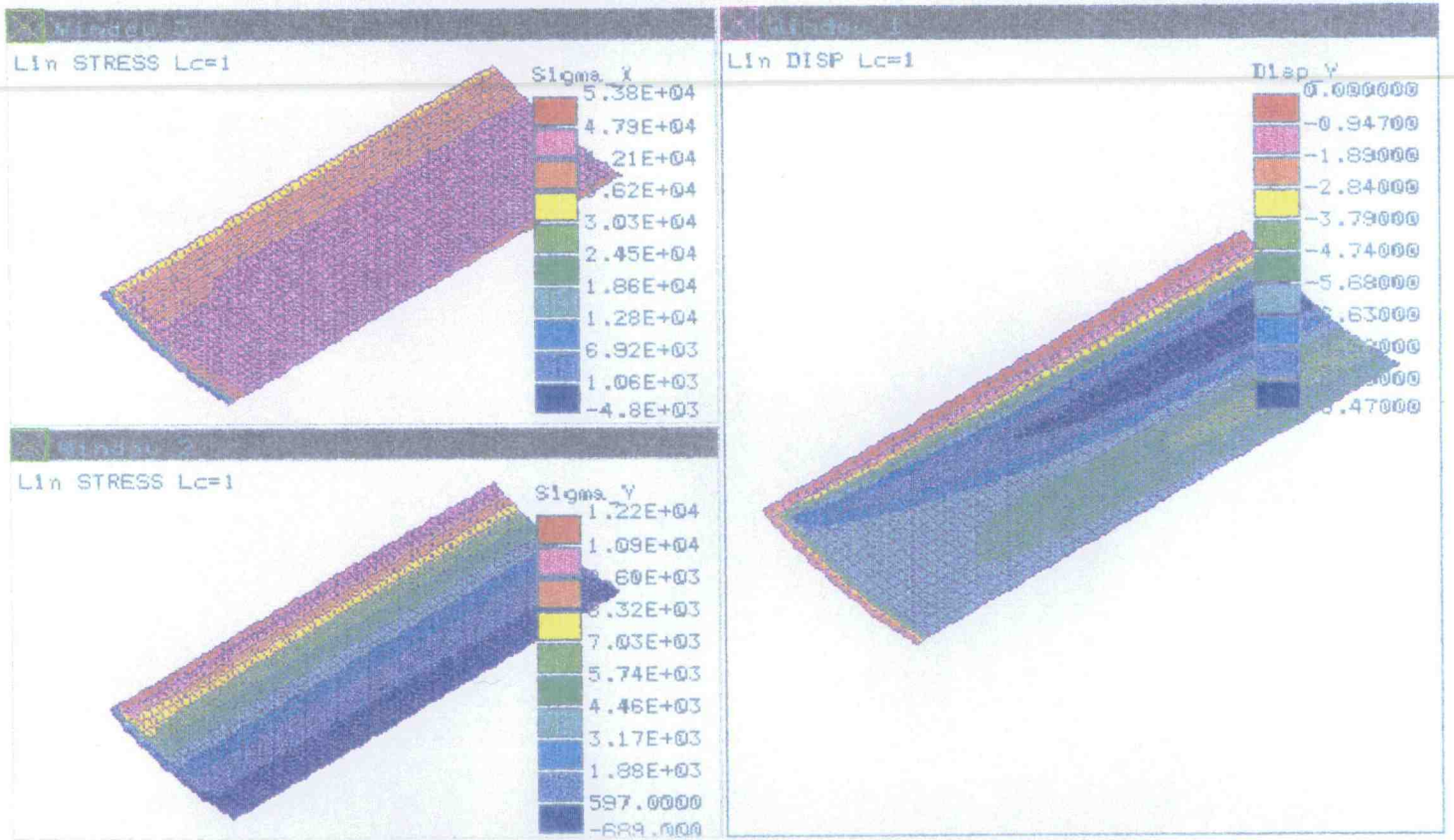

FIGURE 24: STRESS AND DISPLACEMENT PLOTS FOR ARAMID 29/EPOXY BED

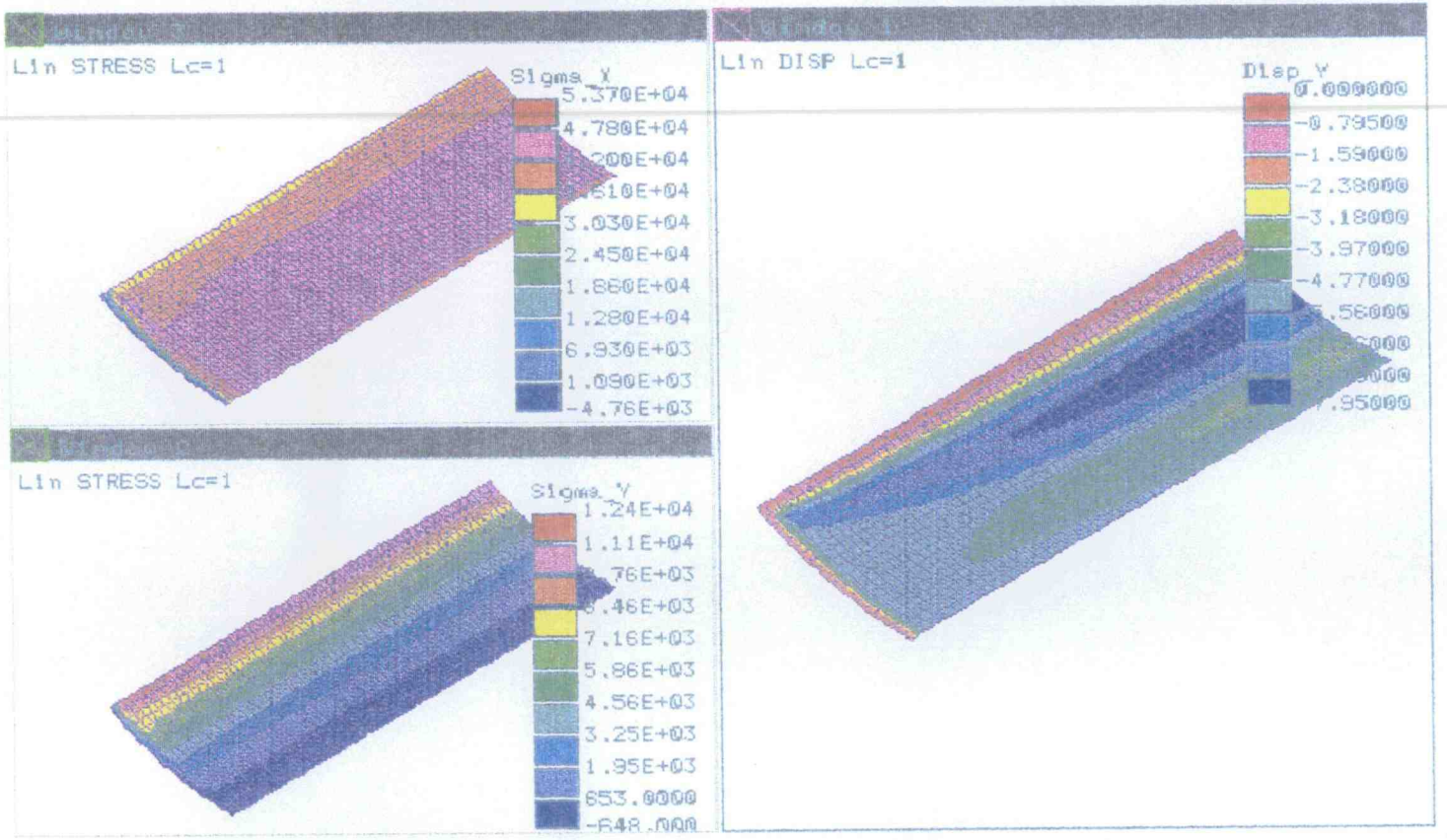

FIGURE 25: STRESS AND DISPLACEMENT PLOTS FOR KEVLAR 49/EPOXY BED

a maximum Sigma Y of 12,200 pounds per square inch at the top of bed, and a maximum displacement of 9.47 inches (figure 24). High value for the displacement of the bed is due to high elongation at break of Kevlar 29 (or Aramid 29) fibers, which is 3.6% [17], nearly fifty percent higher than that of Kevlar 49 fibers. The estimation of the displacement of the bed would, in the final application, help positioning the bed in such a way that there is enough clearance between the bed and the ground-level when the car is fully loaded and is in motion.

The results obtained for Aramid 29/Epoxy bed were compared with those obtained for Kevlar 49/Epoxy. Figure 25 shows the maximum stresses and the Z-direction displacement of Kevlar 49/Epoxy bed. The maximum stress in the X direction is observed to be 53,700 pounds per square inch at the bottom of the bed, and in the Y direction 12,400 pounds per square inch at the top of the bed. The stresses are almost the same in both the material systems, but the displacement of the bed varies. This is because both Kevlar 29 and Kevlar 49 have the same tensile strength, but different elastic moduli. Kevlar 49 is stiffer than Kevlar 29 and hence the Y-displacement obtained for Kevlar 49/Epoxy bed (table 4) is less than the value obtained for Aramid 29/Epoxy bed.

5.2 Microstructure Analysis Results

The microstructure examination of the impregnated fabric samples along the cross-sections AA and BB brought forth distinct differences between Batch 3 and Batch 5 samples. More air-pockets are observed along cross-section AA (figure 26) than along cross-section BB (figure 28) of Batch 5

samples. Air-pockets are observed more in the matrix regions between the fiber crimps, than in that surrounding the fibers in the yarn (figure 30). This suggests that the rolling pressure was inadequate and that there was not enough time for the air-bubbles to escape because of short gelation time.

Void distribution in the case of Batch 3 samples (figure 27 and figure 29) is less pronounced than in the case of Batch 5 samples. Not many air-pockets were noticed in the fiber bundles (figure 31) of Batch 3 samples. It was also observed that there was more resin around the fibers in the case of Batch 3 samples (figure 31) than in the case of Batch 5 samples (figure 30). This suggests that there was sufficient time for the resin to flow in the case of Batch 3 samples.

The void, the resin and the fabric contents in the samples, observed in the microstructures, however, need to be checked with the volume fraction calculations (table 5), because the thickness of the samples is not uniform and the void distribution may vary from one cross-sectional area to the other.

75X

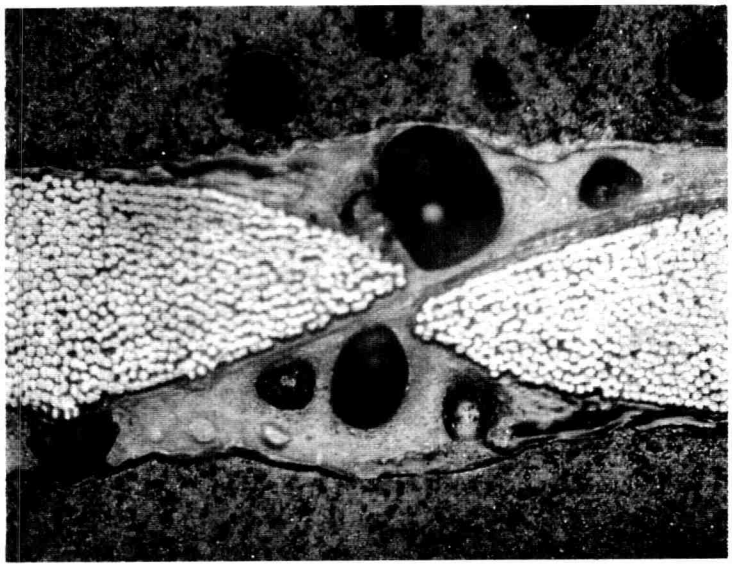

FIGURE 26: PHOTOMICROGRAPH OF BB-CROSS-SECTIONAL VIEW OF BATCH 5 SAMPLES.

75X

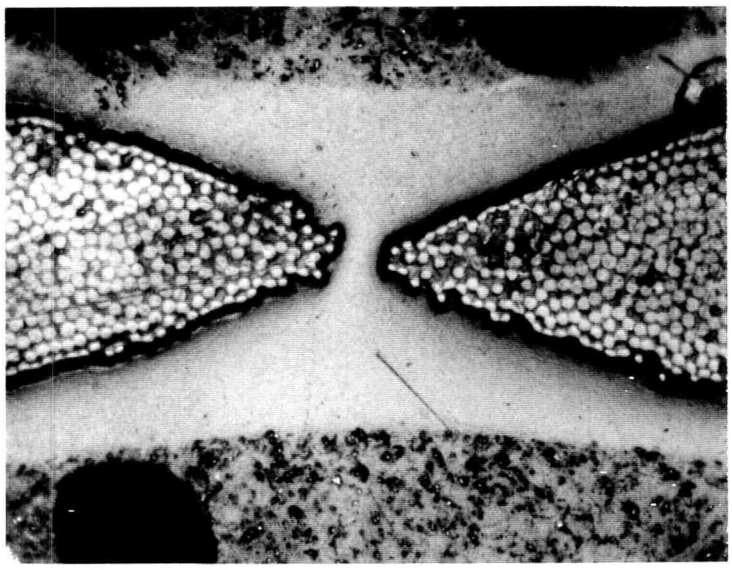

FIGURE 27: PHOTOMICROGRAPH OF BB-CROSS-SECTIONAL VIEW OF BATCH 3 SAMPLES.

75X

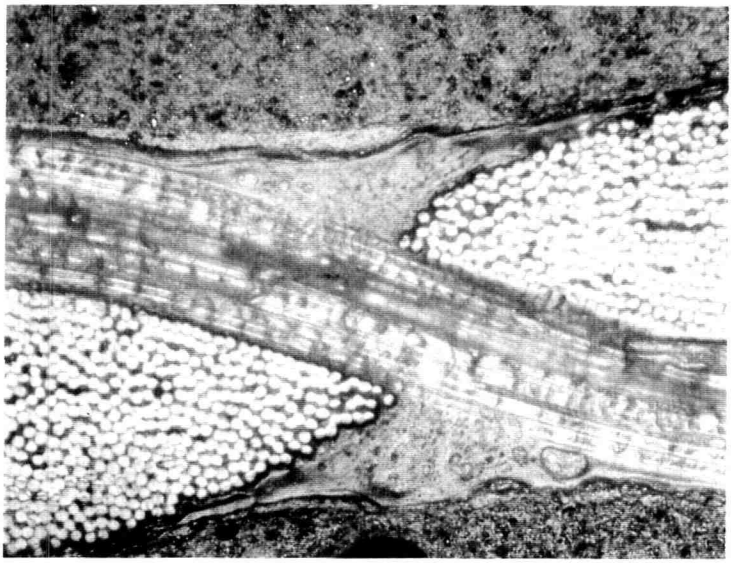

FIGURE 28: PHOTOMICROGRAPH OF AA-CROSS-SECTIONAL VIEW OF BATCH 5 SAMPLES.

75X

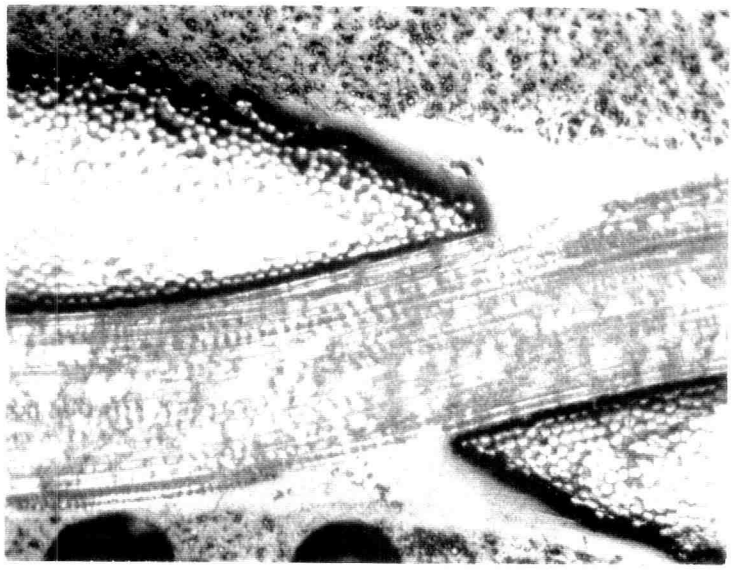

FIGURE 29: PHOTOMICROGRAPH OF AA-CROSS-SECTIONAL VIEW OF BATCH 3 SAMPLES.

400X

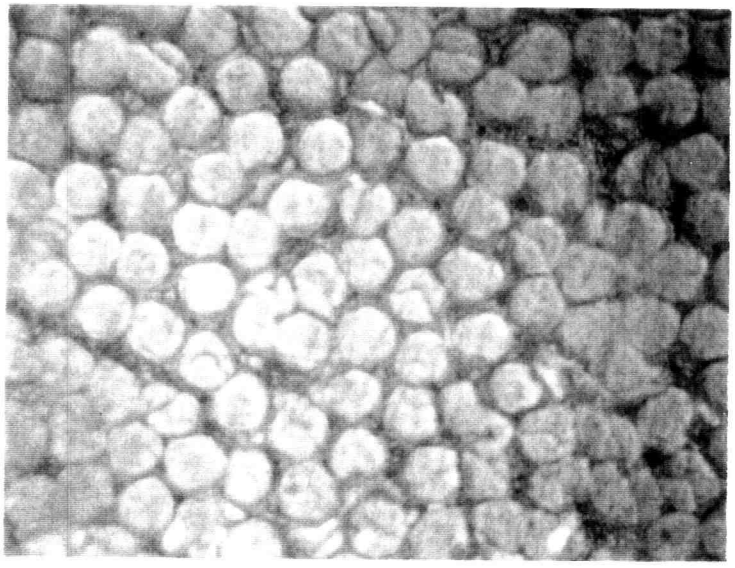

FIGURE 30: PHOTOMICROGRAPH OF FIBER BUNDLE IN THE YARN OF BATCH 5 SAMPLES.

400X

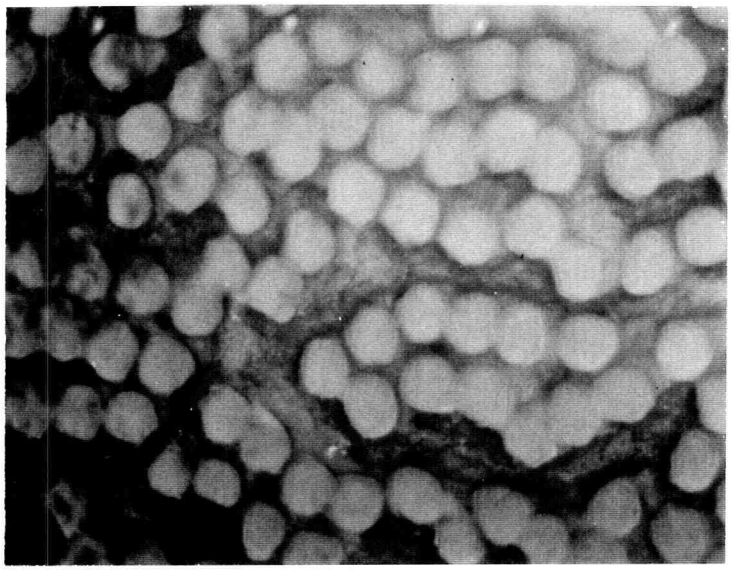

FIGURE 31: PHOTOMICROGRAPH OF FIBER BUNDLE IN THE YARN OF BATCH 3 SAMPLES

5.3 Tensile Strength Characterization

TENSILE STRENGTH OF TEST COUPONS: Table 5 shows the results of the tensile tests performed using wedge grips on the test coupons, impregnated with Uralite using various methods (Batch 1 to Batch 7). In figure 32, it can be observed that the fracture strength of Batch 3-Type coupons is the highest of all the coupons made by other impregnation methods (Batch 1, 2, and 4 to 6). However, the fracture strength of Batch 3-Type coupons is very close to the fracture strength of Batch 4 and 5-Type coupons. Among the coupons impregnated using hand lay-up technique, Batch 3 through Batch 5-Type coupons have higher tensile strength than Batch 1 and 2-Type coupons. This clearly indicates that the viscosity of the

resin system, Uralite 3177, should be reduced further for impregnating a coarse weave (HPF) of denier greater than or equal to 3000 (weaves of denier up to 11500 are available in the market [17]). The viscosity of Uralite is optimum for impregnating NAT (denier 1140).

TABLE 5: TENSILE TEST RESULTS FOR HPF AND NAT COUPONS

Coupons	Min. cross section Area [in.^{2}]	V_{fabric} %	V_{void} %	Mean Fracture Strength [psi]	Min. Fracture Strength [psi]	Max. Fracture Strength [psi]	Std. Devn. [psi]	Coeff of Variation
Unimpregnated HPF	0.0245	--	--	61,665	59,755	63,591	1,461	0.024
Batch 1-Type HPF	0.0266	55.22	7.83	64,113	57,669	69,173	4,273	0.067
Batch 2-Type HPF	0.0266	54.69	7.95	64,586	59,060	66,241	3,102	0.048
Batch 3-Type HPF	0.0266	62.32	4.37	69,368	67,895	71,541	1,435	0.021
Batch 4-Type HPF	0.0266	58.93	6.79	66,739	63,496	69,447	2,690	0.040
Batch 5-Type HPF	0.0266	57.9	3.83	66,917	65,639	67,932	904	0.014
Batch 6-Type HPF	0.0248	67.49	5.83	63,379	60,847	68,145	3,192	0.050
Batch 7-Type NAT	0.0139	24.85	24.6	47,739	43,482	51,187	3,915	0.082

Except Batch 7, all the other impregnation methods resulted in coupons with void content less than 10%. The void content in the case of Batch 7 coupons is approximately 25%. In Batch 7 impregnation method, the painted fabric was left on the nylon sheet for cure (instead of hanging in the air), which entrapped many air bubbles on the bottom of the cured fabric. The Batch 7 coupons also have low fabric content as no pressure was applied in removing the excess resin during the lay-up procedure.

An approximately fifty-five percent (table 5) fabric content and eight percent void content are observed in the Batch 1 and 2-Type hand lay-up coupons. Maximum volume fraction of the fabric is noticed in the case of Batch 3-Type and vacuum-bag (Batch 6) coupons. The higher fabric content in the vacuum-bag coupons is mainly because of the excessive absorption of the resin by the bleeder cloth. Despite the high fabric content, the fracture strength of the vacuum-bag coupons is observed to be much less than that of Batch 1 through Batch 5 hand lay-up coupons. This can be attributed to the yarn (nearly four yarns) pull-outs noticed during the testing of vacuum-bag coupons. This could be because of the poor interfacial strength due to low resin content (approximately twenty-five percent) in the vacuum-bag coupons. A resin content of greater than or equal to thirty-three percent offered good binding force for the fabric and prevented the yarn pull-out during tensile testing.

The tensile test results reveal that the addition of Xylene to the resin mixture (Batch 3 samples) improves the tensile strength of the fabric substantially. Xylene also increases the gelation time of the resin mixture from twenty-four minutes to a little more than forty minutes. The heated resin mixture (Batch 4 and 5-Types) also improves the fracture strength of fabric. However, in the case of Batch 4 and 5-Type impregnation procedures,

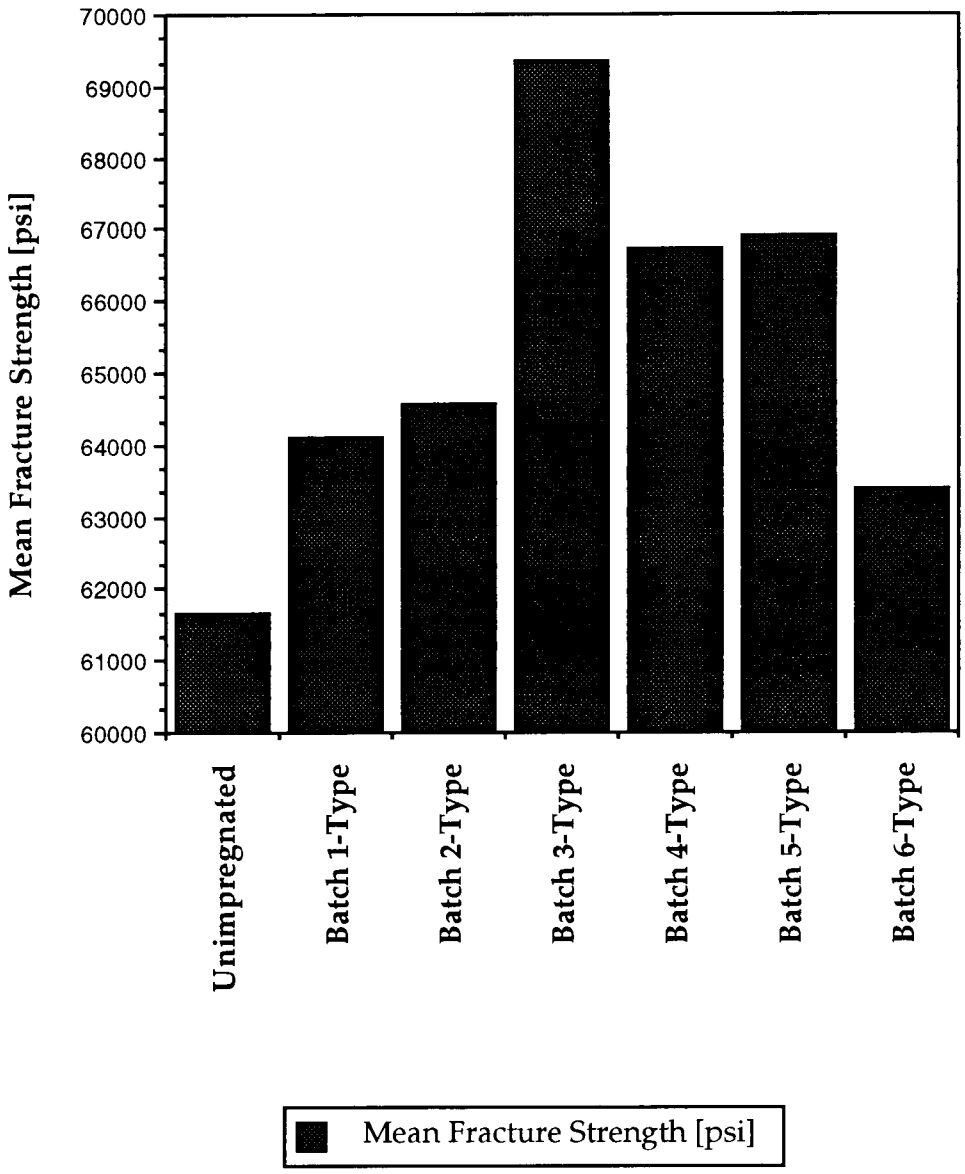

FIGURE 32: TENSILE STRENGTH COMPARISON OF HPF COUPONS

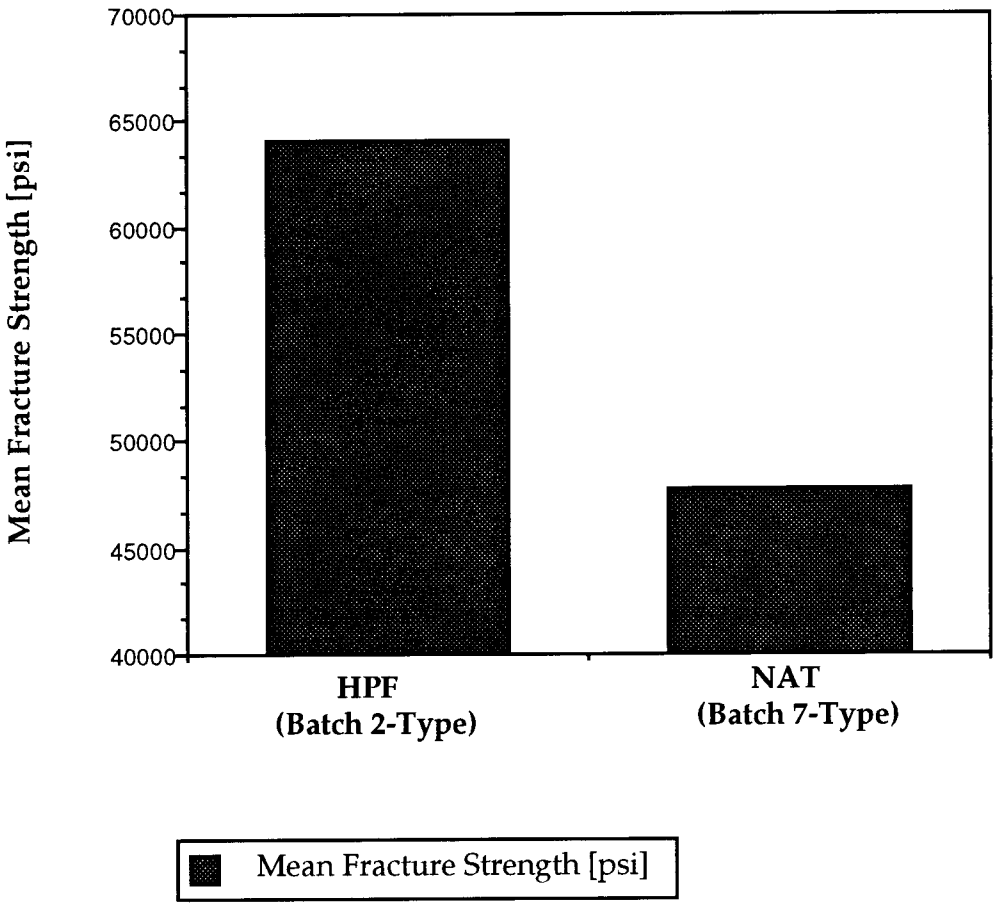

FIGURE 33: TENSILE STRENGTH COMPARISON OF HPF AND NAT

careful planning of the operation is very essential as heating reduces the gelation time of the resin mixture considerably (from twenty-four to five minutes). Painting of just the resin mixture using hand lay-up and vacuum-bag (Batches 1,2 and 6) improved the strength of the fabric marginally. The reason could be high viscosity of the resin for the given fabric (HPF), which is finely woven and has 1333 filaments in each yarn.

GAGE LENGTH EFFECT: Tables 6 and 7 correspond to the results obtained from the tensile tests on increasing gage lengths of HPF coupons. Tables 8 and 9 correspond to the results from tensile tests on NAT. Table 6, 7, and 8 relate to the tests done using wedge grips, whereas table 9 relates to the

TABLE 6: GAGE LENGTH EFFECT TEST (using Wedge Grips) RESULTS FOR UNIMPREGNATED AND BATCH 3-TYPE HPF

Sl. No.	Gage Length [in.]	Fracture Strength [lb./in.^{2}]	
		Unimpregnated HPF	(Batch 3-type)
1.	2.5	61,592	62,669
2.	2.5	66,857	63,271
3.	2.5	65,020	65,075
4.	2.5	65,796	65,075
5.	2.5	66,898	62,406
6.	5.0	64,122	67,143
7.	5.0	59,469	65,489
8.	5.0	60,857	65,188
9.	5.0	60,245	64,323
10.	5.0	63,306	62,782
11.	7.5	61,510	64,323
12.	7.5	60,245	66,203
13.	7.5	61,837	66,729
14.	7.5	59,674	58,835
15.	7.5	63,120	61,015
16.	10.0	52,857	66,203
17.	10.0	54,612	66,880
18.	10.0	53,959	66,692
19.	10.0	52,286	69,135
20.	10.0	51,796	65,902

TABLE 7: GAGE LENGTH EFFECT TEST (using Wedge Grips) RESULTS FOR BATCH 1-TYPE HPF COUPONS

Sl. No.	Gage Length [in.]	Fracture Strength [lb./in.^{2}]
1.	2.5	56,993
2.	2.5	55,639
3.	5.0	65,752
4.	5.0	60,248
5.	7.5	54,887
6.	7.5	61,917
7.	12.5	62,406
8.	12.5	59,248
9.	17.5	56,917
10.	17.5	55,602

TABLE 8: GAGE LENGTH EFFECT TEST (using Wedge Grips) RESULTS FOR NAT

Sl. No.	NAT + EA 9412 (Batch 1-type)		NAT + Uralite (Batch 1-type)	
	Gage Length [in.]	Fracture Strength [lb./in.^{2}]	Gage Length [in.]	Fracture Strength [lb./in.^{2}]
1.	2.5	47,154	2.5	46,971
2.	2.5	46,315	4.0	43,907
3.	4.0	50,215	4.0	56,849
4.	4.0	44,302	5.0	41,727
5.	5.5	42,342	8.5	51,568
6.	5.5	47,383	12.0	48,050
7.	10.5	35,053	13.0	34,907
8.	10.5	43,758	13.0	54,532
9.	13.0	47,664	14.5	47,000
10.	15.5	29,000	18.0	45,640
11.	15.5	46,724	21.0	49,820
12.	21.0	41,604	23.0	50,194
13.	23.5	39,302	23.0	43,130
14.	23.5	43,027	24.0	47,439
15.	24.0	43,081	24.0	44,604

tests done using adapter grips. Figure 34 and table 6 show degradation in the fracture strength with the increase in the gage length of unimpregnated HPF coupons. This is quite consistent with the theoretical background discussed earlier.

A rough estimate of the fracture strength of 360 inches long unimpregnated HPF, can be made using the curve fit equation:

$$Y = 74{,}335 \times X^{-0.12427}.$$

where X is the gage length and Y is the fracture strength of the coupons. This equation, which is a logarithmic curve equation, predicts a fracture strength of 35,780 pounds per square inch approximately.

Excepting coupons tested in the adapter grips (figure 38), all the other impregnated test coupons do not show gage length effect behavior. Scatter in

TABLE 9: GAGE LENGTH EFFECT TEST (using Adapter Grips)
RESULTS FOR NAT

Sl. No.	NAT + Uralite (Batch 1-type)	
	Gage Length [in.]	Fracture Strength [lb./in.^{2}]
1.	1.5	52,690
2.	1.5	57,942
3.	1.5	57,295
4.	5.0	54,201
5.	5.0	49,741
6.	5.0	49,719
7.	9.0	48,547
8.	9.0	43,482
9.	9.0	51,187
10.	13.0	41,396
11.	13.0	44,691
12.	13.0	49,676
13.	20.0	48,525
14.	20.0	49,137
15.	20.0	45,748

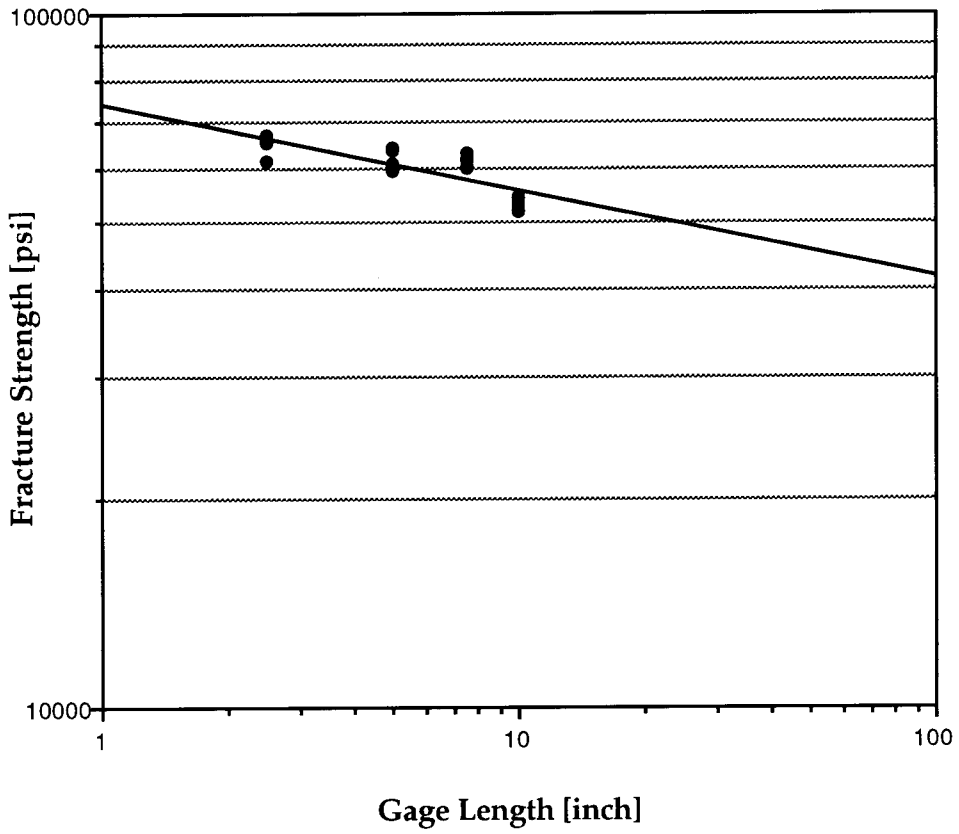

Curve Fit Equation: y = 7.4355e+4 * x^-0.12427

FIGURE 34: GAGE LENGTH VS FRACTURE STRENGTH OF UNIMPREGNATED HPF

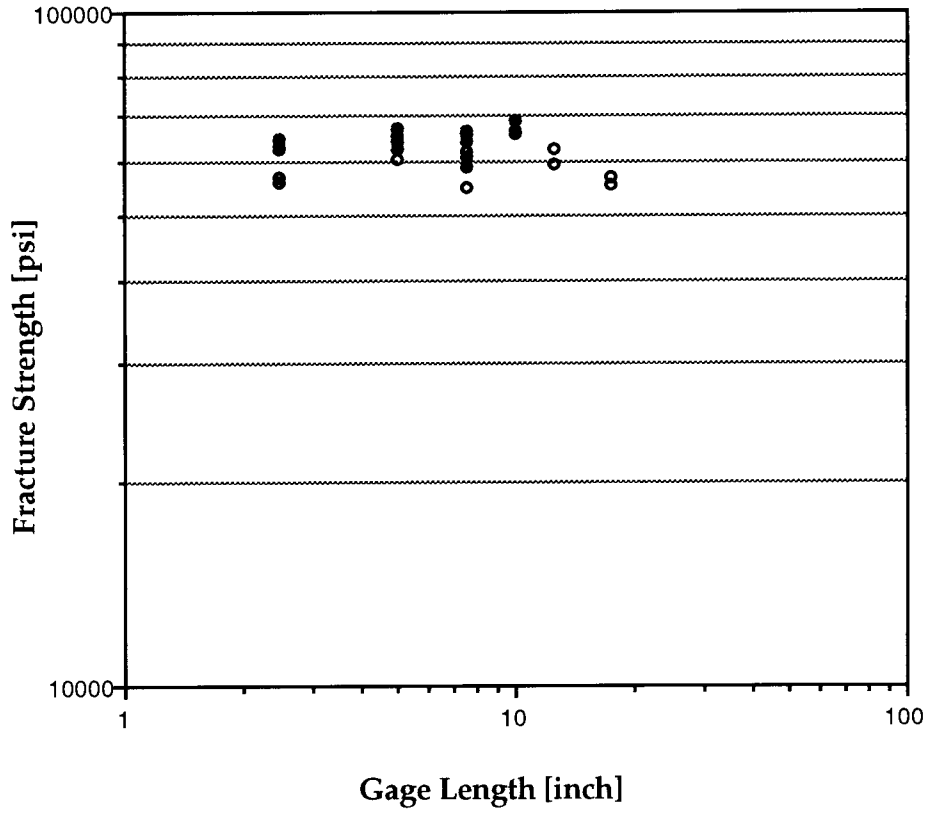

FIGURE 35: GAGE LENGTH VS FRACTURE STRENGTH OF IMPREGNATED HPF

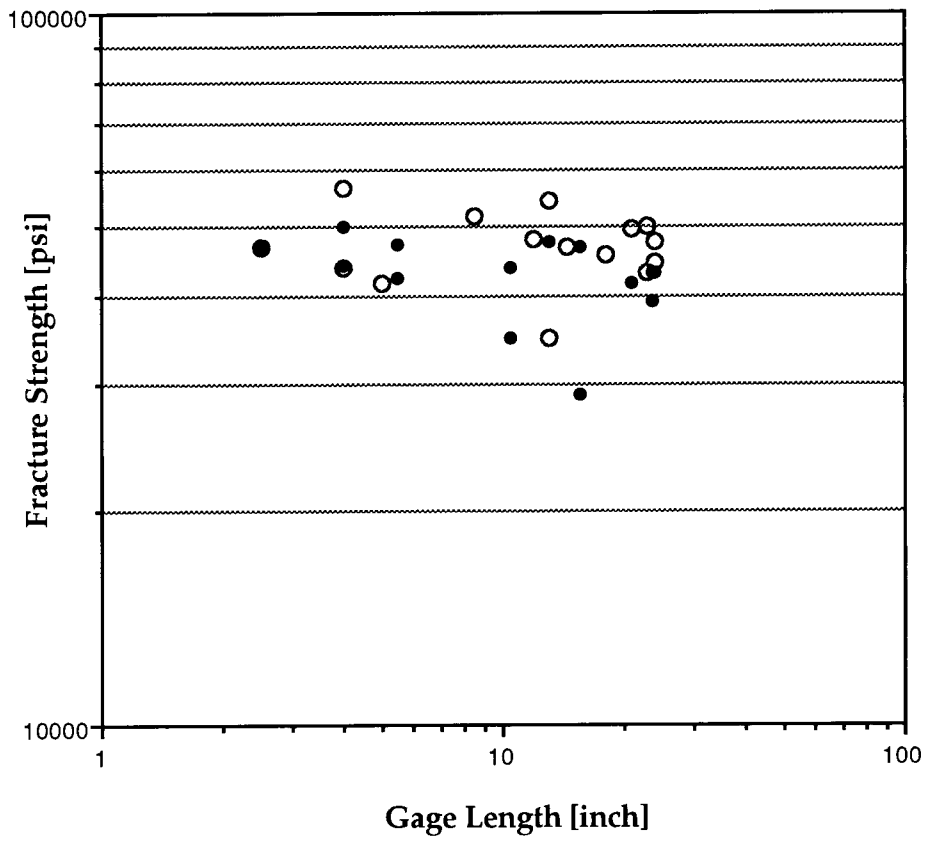

FIGURE 36: GAGE LENGTH VS FRACTURE STRENGTH OF IMPREGNATED NAT

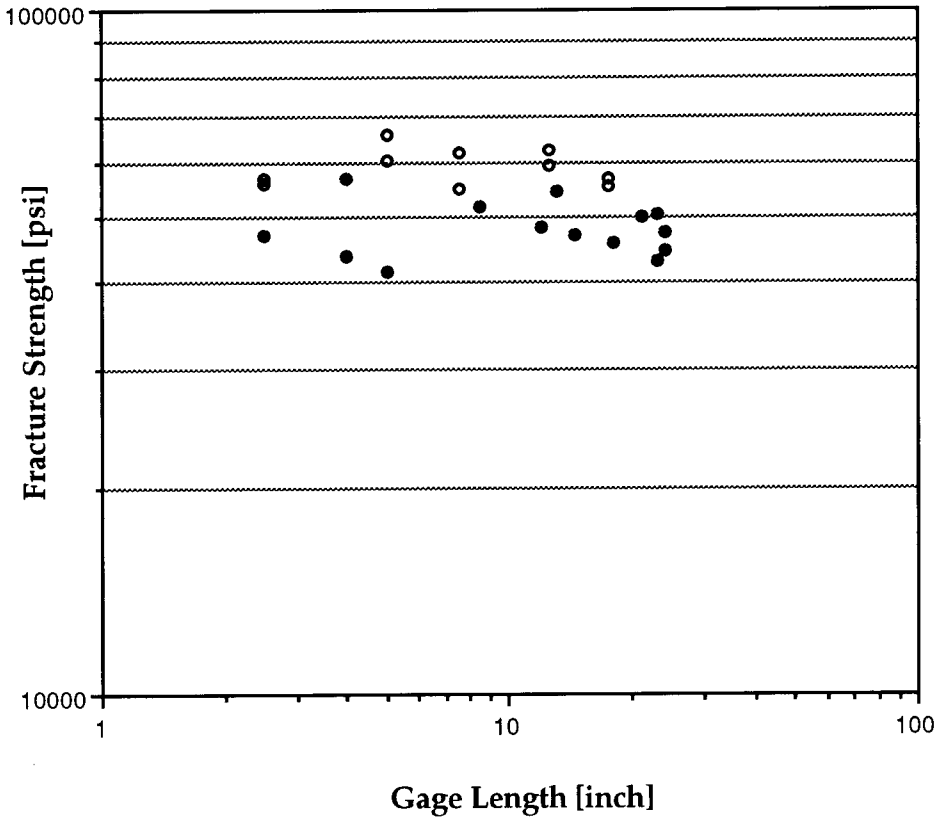

FIGURE 37: GAGE LENGTH VS FRACTURE STRENGTH OF NAT AND HPF

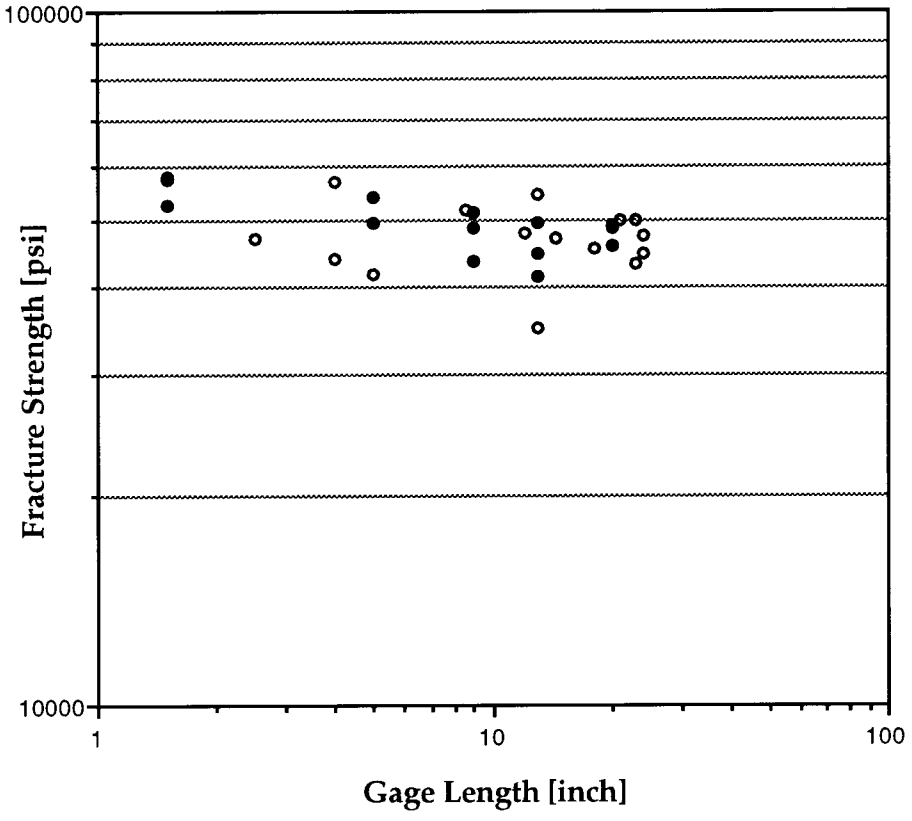

FIGURE 38: GAGE LENGTH VS FRACTURE STRENGTH OF NAT

the fracture strength values is observed for these coupons. The reason that the adapter grip coupons show gage length effect behavior is that the loop section of these coupons was not impregnated with the resin, as it caused delamination of the coupon in the overlap region. The degradation in the strength could be caused by the unimpregnated part of the adapter grip coupons.

Figure 35 shows the tensile test results for Uralite impregnated HPF coupons. For Batch 3-Type HPF coupons, the scatter is noticed in the strength domain, 60,000 to 70,000 pounds per square inch, whereas for Batch 1-Type coupons, it is in the domain, 50,000 to 60,000 pounds per square inch. In figure 36, the test results for epoxy and polyurethane impregnated NAT coupons, the fracture strength of the Uralite impregnated coupons is more stable than that of the epoxy impregnated coupons. In figure 37, the tensile test results for Batch 1-Type HPF and Batch 7-Type NAT, the scatter band for HPF is narrower than that for NAT coupons. Figure 38 shows the gage length effect behavior of adapter grip NAT coupons. The scatter band is the same for both the wedge and the adapter grip NAT coupons.

5.4 Fatigue Test Results

Table 10 gives the fatigue test results for HPF and NAT coupons. Figure 39 shows the results of the room temperature fatigue tests, done on unimpregnated HPF coupons, of gage lengths five and ten inches. The fatigue life decreases with increase in the gage length. This is expected in unimpregnated fabric. Because with the increase in the gage length of fibers the flaws increase. When the fibers in the yarns break, the flaws in the fibers

surrounding the unbroken fibers become the principal sites for the initiation of next break. This continues progressively until failure. The more the flaws, the more the stress concentrated locations, and therefore short fatigue life.

In figure 40, the fatigue behavior of unimpregnated HPF coupons are compared with that of impregnated HPF coupons, of same gage length (ten inches). This is because the unimpregnated coupons have better fatigue life

TABLE 10: FATIGUE DATA FOR HPF AND NAT

Coupon History	Gage Length [in.]	Ultimate Tensile Strength [lb./in.^{2}]	Maximum Stress [lb./in.^{2}]	Cycles to Failure
Unimpregnated HPF	5	61,560	61,500	26,596
			61,357	104,029
			59,549	362,080
			57,740	640,448
Unimpregnated HPF	10	61,665	60,543	390,732
			58,735	353,744
			56,927	999,999
			54,214	1,259,233
			49,694	5,062,777
Batch 5-Type HPF	10	66,917	58,261	14,266
			54,098	16,330
			52,432	126,278
			49,934	2,316,213
			45,771	5,862,000
Batch 6-Type HPF	10	63,379	59,811	3841
			58,024	8133
			56,238	47,609
			53,559	83,687
			49,093	1,540,405
Batch 1-Type NAT	5	47,739	46,068	1,362
			45,352	1,617
			44,875	52,669
			43,920	544,518
			43,443	762,439
			40,578	3,435,000

than the impregnated coupons. The impregnated coupons have air pockets in addition to the flaws in the fibers. Besides, the resin matrix provides a medium for the crack to propagate.

Not much difference in the fatigue behavior is noticed in the case of Batch 5-type and Batch 6-Type coupons, as shown in figure 41. However, a great difference in fatigue life is noticed in the Uralite impregnated coupons of NAT and HPF. This is because of higher percentage of imperfections in the impregnated NAT coupons (void content of approximately twenty-five percent) than in the impregnated ones.

The fatigue data for Batch 5-type HPF coupons are used to predict the stress level, below which the coal support-bed can serve without failure for ten years, under a dynamic load at a frequency of 25 HZ. The maximum cycles the coal support-bed has to endure without failure is calculated to be approximately 3.2E+09 cycles. The curve fit equation, which gave closer approximations to the test data, is

$$Y = 68{,}219 \times X^{-0.022584}$$

where X is the number of cycles and Y is the maximum stress on the coupons. The minimum stress, predicted by this equation, is 41,628 pounds per inch which is approximately sixty-one percent of the mean fracture strength of the Batch 5-Type HPF coupons.

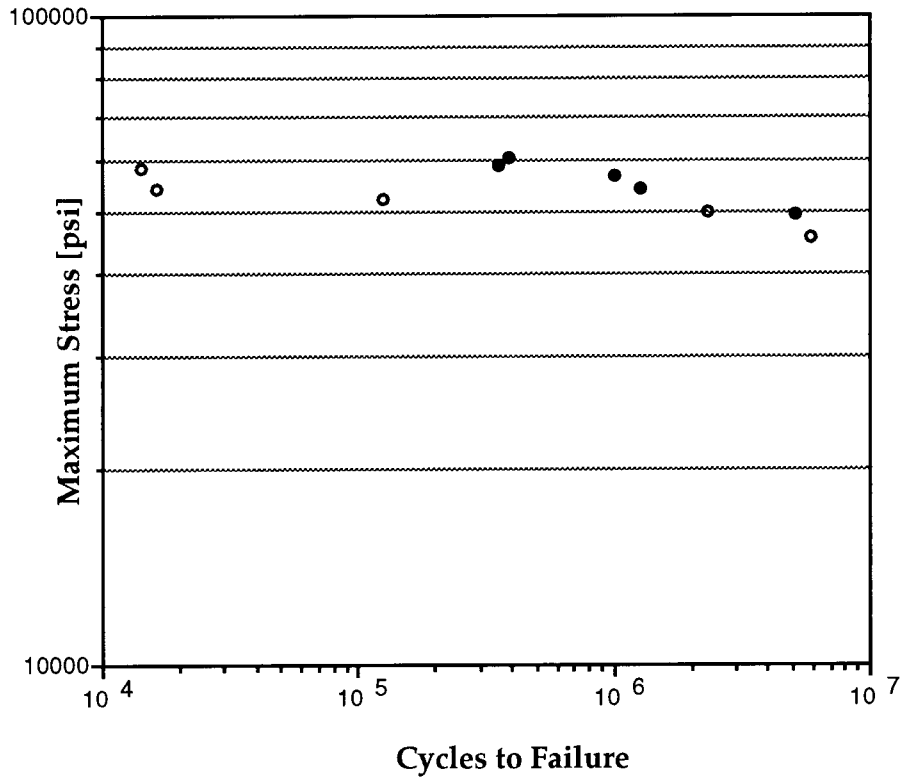

FIGURE 39: MAXIMUM STRESS VS CYCLES TO FAILURE FOR UNIMPREGNATED HPF

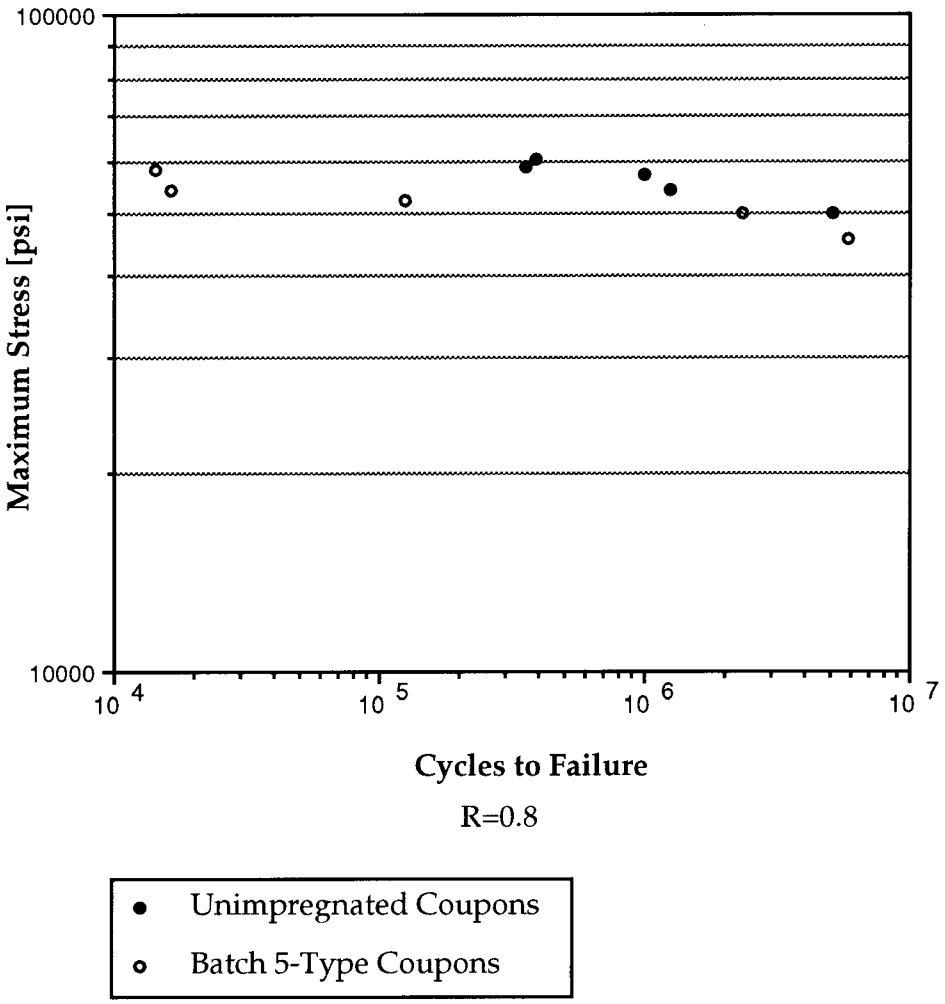

FIGURE 40: MAXIMUM STRESS VS CYCLES TO FAILURE FOR HPF

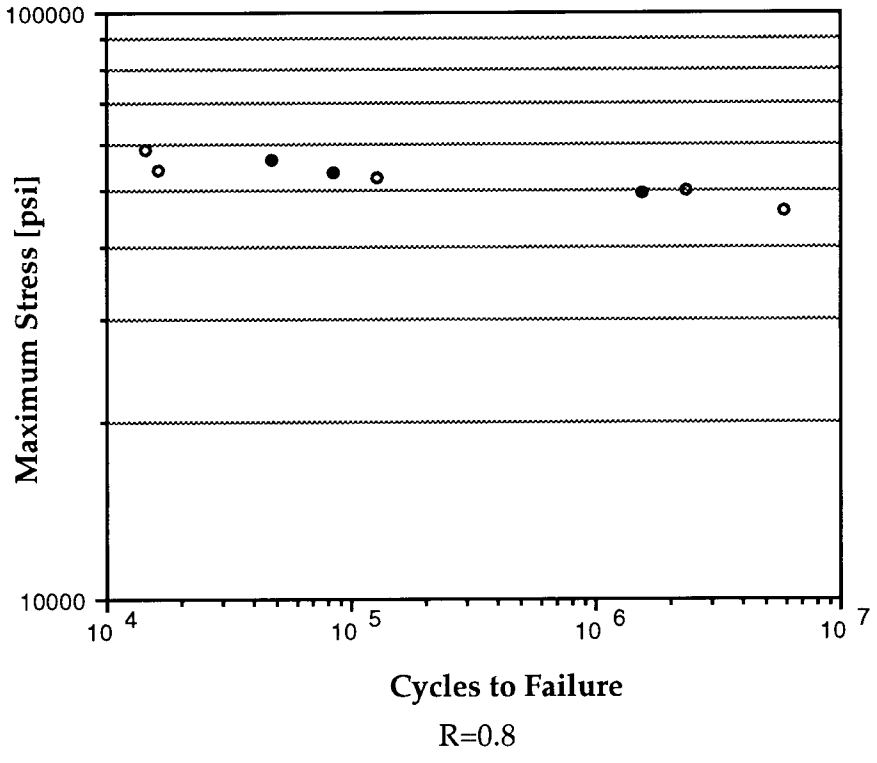

FIGURE 41: MAXIMUM STRESS VS CYCLES TO FAILURE FOR HPF

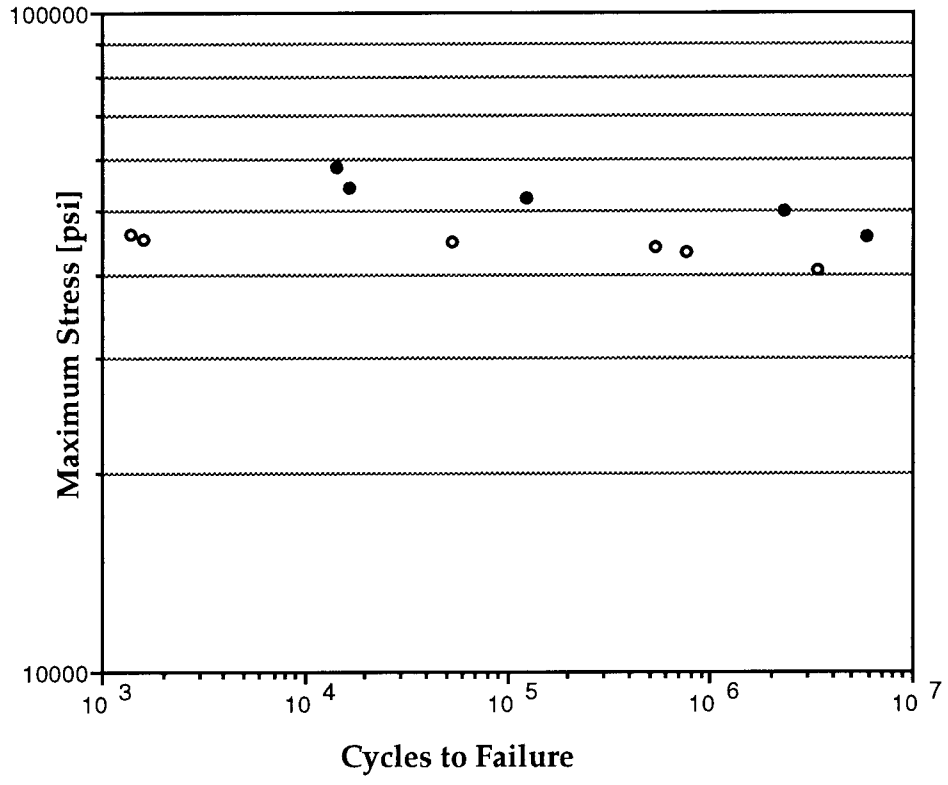

FIGURE 42: MAXIMUM STRESS VS CYCLES TO FAILURE FOR HPF AND NAT

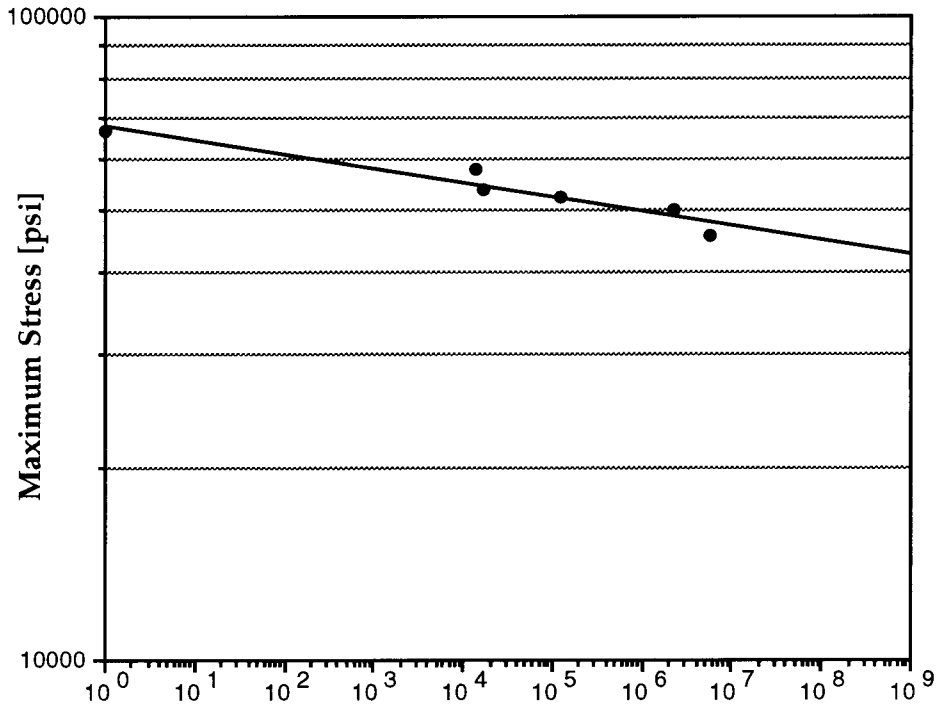

Curve Fit Equation: y = 6.8219e+4 * x^-2.2584e-2

FIGURE 43: MAXIMUM STRESS VS CYCLES TO FAILURE FOR BATCH-5 TYPE HPF

5.5 Chemical Resistance of Impregnated Fabric

Table 11 presents the results of tensile tests done on Batch 5-Type coupons of gage length ten inches, after immersing in acidic and basic aqueous solutions. It can be observed in table 11, and figures 44 and 45, that

TABLE 11: CHEMICAL RESISTANCE TEST DATA FOR HPF

Sl. No.	Temperature ° F	Time (Hours)	pH	Fracture Strength [lb./in.
1.	122	30	2	60,865 59,624 59,286 61,128 54,925
2.	122	75	2	58,271 57,594 58,872 58,684 58,496
3.	122	115	2	54,474 56,015 57,068 55,489 58,722
4.	122	75	5	58,384 54,925 54,323 53,647 59,774
5.	122	75	11	61,353 60,940 60,602 63,835 58,797
6.	212	10	2	53,008 49,850 49,850 54,323 43,496

the Uralite impregnated HPF coupons retain eighty-seven percent of their initial tensile strength after seventy-five hours of immersion in an aqueous solution of sulfuric acid with pH less than or equal to five. In an aqueous solution of caustic base; ammonium hydroxide, Batch 5-Type HPF coupons retain ninety percent of its initial strength.

Figure 45 shows a decrease in the strength of the impregnated coupons, immersed in aqueous sulfuric acid solution, with time of exposure. The decrease in the fracture strength of the coupons after 115 hours of immersion is noted to be sixteen percent of the initial strength.

At an elevated temperature of 122°F, after ten hours of immersion in a ten percent concentrated sulfuric acid solution, the strength loss is observed to be nineteen percent to thirty-five percent. Du Pont [17] reports an appreciable strength loss of forty-one to eighty percent for unimpregnated Kevlar aramid yarn in the similar conditions. This implies that the impregnation improves the chemical resistance of the fabric.

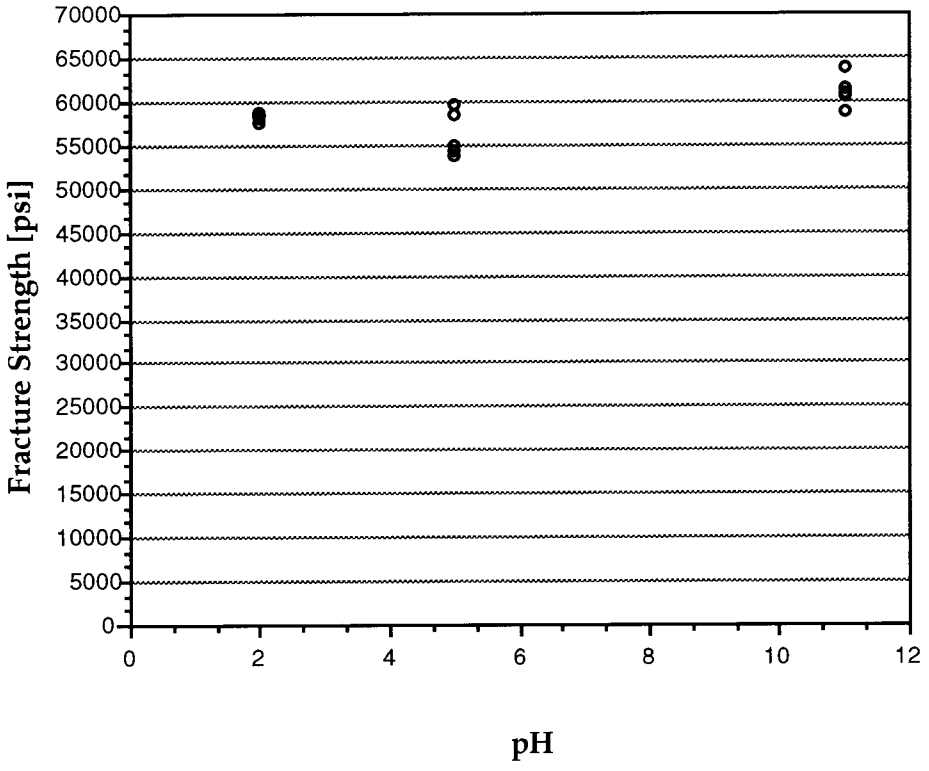

Curve Fit equation: y = 6.1543e+4 - 1922.1x + 171.12x^2

FIGURE 44: pH VS FRACTURE STRENGTH OF BATCH 5-TYPE HPF

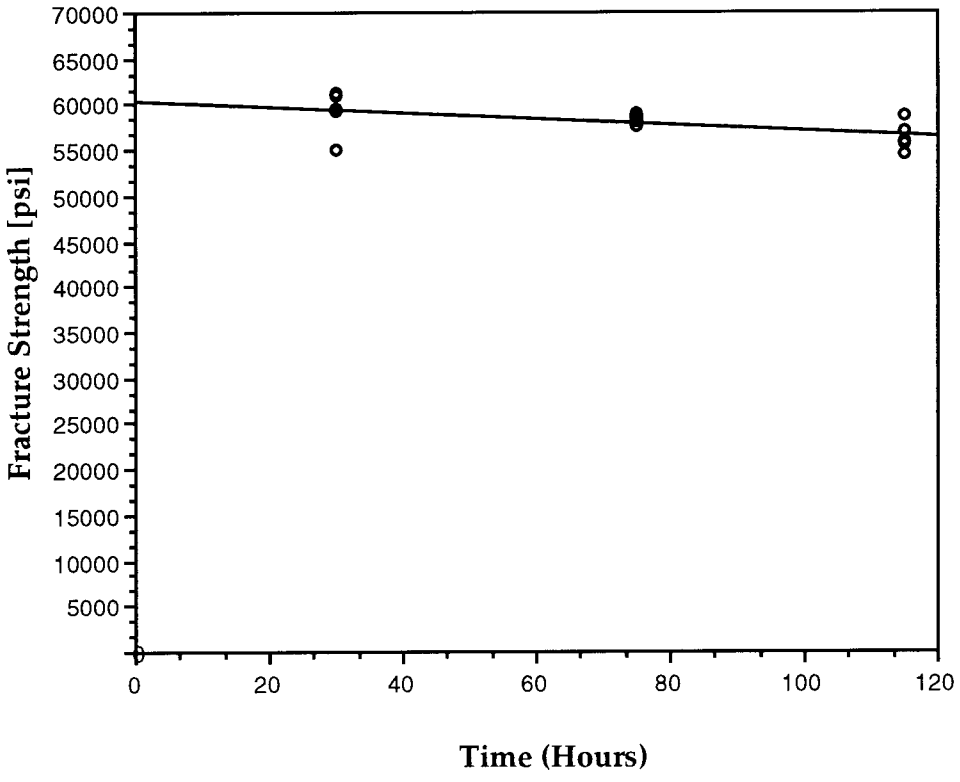

Curve Fit equation: y = 6.0370e+4 - 32.757x

FIGURE 45: TIME VS FRACTURE STRENGTH OF BATCH 5-TYPE HPF IN pH 2 SOLUTION

6. CONCLUSIONS

All the impregnation procedures adopted in this study improved the fracture strength of the fabric. Batch 3 impregnation method yielded coupons with the highest fracture strength (69,368 psi), whereas Batch 7 yielded coupons with the lowest strength (63,379 psi).

The maximum in-plane stress developed in the bed due to the weight of coal (a factor of safety 2 on static load of 240,000 pounds) is determined to be 53,800 pounds per square inch, which is approximately 85% of the mean strength of Batch 6-Type coupons. But fatigue test results show 61% of the mean fracture strength as the endurance limit for safe operation of the bed over a service life of ten years. This suggests the need for a Kevlar 29 fabric with higher strength, at least 2390 pounds per inch.

Addition of Xylene to the resin mixture (Batch 3 impregnation procedure), before applying on the Kevlar 29 fabric using hand lay-up technique, enhances the strength of the fabric. This procedure also extends the gelation time; therefore more time is available for the impregnation process as well as for the resin to flow into the fibers of the fabric. Batch 3 and Batch 5 impregnation procedures yielded coupons with the least void content, approximately 4%.

A gage length effect is not observed in the impregnated fabric, whereas it is observed in the unimpregnated fabric. More degradation in the strength of the polyurethane impregnated fabric occurs in the acidic medium than in the basic medium. The degradation of mechanical properties increases with time. After immersion in an aqueous sulfuric acid (pH 2) for approximately five days, an approximately fourteen percent decrease in the fracture strength

of the polyurethane impregnated fabric (Batch 5-Type coupons) is observed. The strength loss of the impregnated fabric (19% to 35%) is less than that of the unimpregnated yarn (41% to 80%) [17] after ten hours of immersion in a ten percent concentrated sulfuric acid solution at 122°F. To be able to predict the strength loss in sulfuric acid solution over the service life of the bed, future research should involve testing the impregnated coupons for tensile strength after longer immersion times (at least a month).

7. RECOMMENDATIONS FOR FUTURE RESEARCH

1. Future research should involve testing Batch 3-Type fabric coupons for abrasion and impact resistance. If the polyurethane impregnated fabric has to be improved for abrasion resistance, the alumina powder or cement powder mixed with the polyurethane or an acid resistant resin matrix should be co-cured with the impregnating resin matrix. The co-curing of the impregnating resin mixture and alumina coating mixture will prevent delamination of the alumina coating from the impregnated fabric.

2. Further research needs to be undertaken in the area of clamping mechanisms for the coal support-bed. Modifications on the fabrication procedures for adapter grip coupons should involve impregnating the loop section of the coupon to prevent the gage length effect.

3. Fatigue tests need to be conducted in a temperature controlled environmental chamber. The fatigue life of coated fabric should be determined at very low (-50°F) and elevated (300°F) temperatures, as the temperature range in which the coal support-bed is expected to serve is -50 to 300°F.

4. Analysis of the dynamic loads; impact and fatigue, besides the static load, using COSMOS, will help predicting accurately the stresses develped in the coal support bed.

8. REFERENCES

1. T. C. KENNEDY and N. MEAD, "Finite Element Analysis of a Composite Steel/Aluminum Coal Car", Final Report for Oregon Metals Initiative (OMI) project, July 1991.

2. FRANK SCARDINA, "An Introduction to Textile Structures and their Behavior", Textile Structural Composites, TSU-WEI-CHOU and FRANK K. KO, Editors, Elsevier Science Publishers, NewYork, 1989, pp. 5.

3. H. W. REINHARDT, "On the Biaxial Testing and Strength of Coated Fabrics" *Experimental Mechanics,* 1976, pp. 71-74.

4. N. STUBBS, "Elastic and Inelastic Response of Coated Fabrics to Arbitrary Loading Paths" , Textile Structural Composites, TSU-WEI-CHOU and FRANK K. KO, Editors, Elsevier Science Publishers, NewYork, 1989, pp. 331-353.

5. R. J. MORGAN and R. E. ALLRED, Reference Book for Composite Technology, Technomic Publishing Co., Inc., Lancaster, PA, 1989, pp. 143-163.

6. Du Pont, A Preliminary Information Memo, "Characteristics and Uses of Kevlar 29 Aramid", September 28, 1976.

7. T. W. CHOU and T. ISHIKAWA, "Analysis and Modeling of two-dimensional fabric composites", Textile Structural Composites, T. W. CHOU and FRANK K. KO, Editors, Elsevier Science Publishers B. V., Amsterdam, 1989, pp. 209-264.

8. University of Delaware, Center for Composite Materials, "Woven Fabric Micromechanics", Technomic Publication Co., 1991, IBM software for PC.

9. K. K. CHAWLA, Composite Materials, Springer-Verlag New York Inc., 1987, pp. 89-91.

10. "Fabrication Techniques for Advanced Reinforced Plastics", Symposium: 22/23 April 1980, University of Salford, UK, pp. 27.

11. C. ZWEBEN, *Journal of Materials science*, Vol. 12, No. 7, 1977, pp. 1325-1337.

12. C. ZWEBEN, W. S. SMITH and M. W. WARDLE, "Test Methods for Fiber Tensile Strength, Composite Flexural Modulus, and Properties of Fabric Reinforced Laminates", Composite Materials, Testing and Design (Fifth Conference), ASTM STP 674, S. W. TSAI, Editor, American Society for Testing and Materials, 1979, pp. 228-262.

13. M. J. SALKIND, "Fatigue of Composites", Composite Materials, Testing and Design (second Conference), ASTM STP 497, American Society for Testing and Materials, 1972, pp. 143-169.

14. P. W. M. PETERS and K. SCHULTE, "Polymer Matrix Composites", Advanced Aerospace Materials, H. BUHL, Editor, Springer-Verlog Berlin, Heidelberg 1992, pp. 238-239.

15. CH. BARON, K. SCHULTE, H. HARIG, Composite Science and Technology, vol. 29, 1987, pp.257.

16. E. A. NEWELL ARBER, The Natural History of Coal, Cambridge University Press, 1911.

17. Du Pont Technical Guide, "Kevlar Aramid Fiber", December 1992.

18. ASTM standard D3039/D3039M-93, "Standard Test Method for Tensile Properties of Polymer Matrix Composite Materials", Annual Book of ASTM Standards, 1993.

19. ASTM Standard D792-91, "Standard Test Methods for Density and Specific Gravity (Relative Density) of Plastics by Displacement", Annual Book of ASTM Standards, 1991.

20. ASTM Standard D2734-91, "Standard Test Methods for Void Content of Reinforced Plastics", Annual Book of ASTM Standards, 1991.

21. ASTM Standard D3479-76, "Standard Test Methods for Tension-Tension Fatigue of Oriented Fiber, Resin Matrix Composites", Annual Book of ASTM Standards, 1976.

22. N. L. HANCOX, "High Performance Composites with Resin Matrices", Handbook of Composites, Vol. 4, Fabrication of Composites, A. KELLY and S. T. MILEIKA, Editors, Elsevier Science Publishers B. V., 1983, pp. 1-44.

23. CARL ZWEBEN, " Tensile Failure of Fiber Composites ", *AIAA Journal*, vol. 6, December 1968.

24. B.WALTER ROSEN, " Tensile Failure of Fibrous Composites ", *AIAA Journal* , vol. 2, No. 11, November 1964.

25. C. ZWEBEN and B.W. ROSEN, "A Statistical Theory of Material Strength with Application to Composite Materials", *Journal of Mechanics of Physics and solids*, vol. 18, 1970, pp. 189-206.

26. JAMES D. PILEGGI, Gunderson Inc., Private Communication.

27. C. HEPBURN, Polyurethane Elastomers, Applied Science Publishers Ltd., England, 1982.

28. R. W. DYSON, Editor, Engineering Polymers, Blackie & Son Limited, London, 1990.

29. HANS-GEORG ELIAS, New Commercial Polymers 1969-1975, Gordon and Breach Science Publishers, Inc., New York.

APPENDIX 1: COSMOS INPUT FILE FOR KEVLAR 49/EPOXY BED

```
C* COSMOS/M     Geostar V1.65A
C* Problem : KEV29          Date : 10-MAR-94  Time : 16:34:40
C**********************************************
PT,1,0,0,0,
PT,2,0,0,-180,
PT,3,-57.5,14.673,-180,
PT,4,-57.5,14.673,0,
PT,5,-28,14,0,
PT,6,-28,14,-180,
SCALE,0,
CRARC,1,4,1,5,120,
CRLINE,2,1,2,
CRARC,3,2,3,6,120,
CRLINE,4,3,4,
PTDEL,5,6,1,
CLS,1,
SF4CR,1,1,2,3,4,0,
EGROUP,1,SHELL4L,1,1,0,0,0,0,0,
MPROP,1,EX,0.179E+07,
MPROP,1,EY,0.113E+07,
MPROP,1,NUXY,0.0763,
MPROP,1,GXY,0.29E+06,
RCONST,1,1,1,5,0.014,0,0.028,1,0,
CLS,1,
SFREORNT,1,1,1,
SFREPAR,1,2,
M_SF,1,1,1,4,60,20,1,1,
NMERGE,1,1281,1,0.0001,0,1,0,
CLS,1,
DCR,1,UX,0,4,3,UY,UZ,RX,RY,RZ,
DCR,2,UX,0,2,1,RY,RZ,,
DCR,3,UZ,0,3,1,RX,RY,,
PSF,1,11.118,1,1,11.118,11.118,
CLS,1,
```

APPENDIX 2: COSMOS INPUT FILE FOR KEVLAR 29/EPOXY BED

```
C* COSMOS/M     Geostar V1.65A
C* Problem : KEV29          Date : 10-MAR-94  Time : 16:34:40
C*********************************************
PT,1,0,0,0,
PT,2,0,0,-180,
PT,3,-57.5,14.673,-180,
PT,4,-57.5,14.673,0,
PT,5,-28,14,0,
PT,6,-28,14,-180,
SCALE,0,
CRARC,1,4,1,5,120,
CRLINE,2,1,2,
CRARC,3,2,3,6,120,
CRLINE,4,3,4,
PTDEL,5,6,1,
CLS,1,
SF4CR,1,1,2,3,4,0,
EGROUP,1,SHELL4L,1,1,0,0,0,0,0,
MPROP,1,EX,0.17E+07,
MPROP,1,EY,0.949E+06,
MPROP,1,NUXY,0.0679,
MPROP,1,GXY,0.363E+06,
RCONST,1,1,1,5,0.014,0,0.028,1,0,
CLS,1,
SFREORNT,1,1,1,
SFREPAR,1,2,
M_SF,1,1,1,4,60,20,1,1,
NMERGE,1,1281,1,0.0001,0,1,0,
CLS,1,
DCR,1,UX,0,4,3,UY,UZ,RX,RY,RZ,
DCR,2,UX,0,2,1,RY,RZ,,
DCR,3,UZ,0,3,1,RX,RY,,
PSF,1,11.118,1,1,11.118,11.118,
CLS,1,
```

APPENDIX 3: WFM OUTPUT FOR KEVLAR 49/EPOXY FABRIC

LAMINA PROPERTIES

1. E1 = .110E+08
2. E2 = .800E+06
3. G12 = .330E+06
4. NU12 = .340E+00
5. NU23 = .380E+00
6. AL1 = -.222E-05
7. AL2 = .439E-04

MATRIX PROPERTIES

1. EM = .499E+06
2. GM = .185E+06
3. NUM = .350E+00
4. ALM = .320E-04

GEOMETRICAL INPUT

1. ng = .200E+01
2. Laminate Thickness = .280E-01
3. Height of Fabric excluding matrix = .250E-01
4. Total length of repeating unit = .590E-01
5. Length of undulated region = .550E-01

CALCULATED EFFECTIVE PROPERTIES

1. EX = 0.179E+07
2. EY = 0.113E+06
3. GXY = 0.290E+06
4. NUXY = 0.763E-01

APPENDIX 4: WFM OUTPUT FOR KEVLAR 29/EPOXY FABRIC

LAMINA PROPERTIES

1. E1 = .725E+07
2. E2 = .725E+06
3. G12 = .435E+06
4. NU12 = .222E+00
5. NU23 = .250E+00
6. AL1 = -.222E-05
7. AL2 = .439E-04

MATRIX PROPERTIES

1. EM = .499E+06
2. GM = .185E+06
3. NUM = .350E+00
4. ALM = .320E-04

GEOMETRICAL INPUT

1. ng = .200E+01
2. Laminate Thickness = .280E-01
3. Height of Fabric excluding matrix = .250E-01
4. Total length of repeating unit = .590E-01
5. Length of undulated region = .550E-01

CALCULATED EFFECTIVE PROPERTIES

1. EX = 0.170E+07
2. EY = 0.949E+06
3. GXY = 0.363E+06
4. NUXY = 0.679E-01